ISSN 0252-1075
Contribution from IITM
Research Report No. RR-113

An Objective Study of Indian summer Monsoon Variability Using the Self Organizing Map Algorithms

A.K. Sahai
and
R. Chattopadhyay

July 2006

Indian Institute of Tropical Meteorology
Dr. Homi Bhabha Road, Pashan Pune - 411 008
Maharashtra, India

E-mail : lip@tropmet.res.in Fax : 91-020-25893825
Web : http://www.tropmet.res.in Telephone : 91-020-25893600

CONTENTS

An Objective Study of Indian summer Monsoon Variability Using the Self Organizing Map Algorithms

A.K. Sahai and R. Chattopadhyay
Indian Institute of Tropical Meteorology, Pune

ABSTRACT

The Intraseasonal Oscillations (ISO) of the Indian Summer Monsoon (ISM) has been classified traditionally in terms of active and break phases after the onset around the end of May or early June. Such phases of monsoon are characterized by distinct synoptic features associated with precipitation and various other meteorological parameters. Here we make an attempt of objective classification of the synoptic patterns of precipitation in terms of the following dynamical parameters: large scale circulation indices viz. vertical zonal wind shear index (Webster and Yang, 1992), vertical meridional wind shear index (Goswami et al. 1999) and meridional shear of zonal wind index (Wang and Fan, 1999), mean sea level pressure (MSLP), specific humidity at 850mb (SPH) and geopotential height at 500mb (GPH). The data used in this study was obtained from ERA-40 data set (http://www.ecmwf.int/research/era/). The classification is obtained using Kohenen's Self Organizing Map (SOM) algorithms. The most important advantage of SOM is that we don't fix any pre-defined criterion to determine the values of parameters in identification of active and break states; instead various states evolve interacting non-linearly in such a way that very dissimilar states are widely separated and transitional states are placed between the groups. In this study the ISOs are classified using 3x3 SOM states. When compared for precipitation, it is found that 3 of them belong to active (with one wettest), 3 to break (with one driest) and remaining 3 belong to normal conditions. The composite spatial patterns of these states showed that the active and break states of precipitation and their transition are well captured with the above mentioned parameters. The states characterized as wettest and driest patterns were considered further to obtain objective classification of active and break spells. Using the proposed criteria (Table 2) 42 active and 37 break spells were identified during 1980-2001 period. The spatial pattern of composite break and active spells matches well with earlier studies and with other observations. This shows that any general circulation model which captures the spatial and temporal variability of large scale circulation, humidity, pressure during the monsoon season may well forecast the rainfall. The other important results are:

The study shows that the multi-scale non linear interactions among large scale circulation (represented by circulation indices) and local convection (represented by MSLP, GPH and SPH) play the key role in the monsoon precipitation.

A significant correlation of break state with El-Nino condition can be seen from the study.

There is a systematic transition pattern from one state to the other with higher staying probability at the most active and break states.

Introduction

The monsoon season over Indian subcontinent has an age-old tradition of synoptic classification. Such synoptic grouping is based on numerous observations by meteorologists for over a century (one of the earliest reference being Blanford, 1986). The synoptic charts and the experience of many renowned meteorologists lead to a satisfying and simpler classification of monsoon (Malurkar 1950; Ramamurthy 1969; Raghavan 1973; Krishnamurthy and Bhalme 1976; Alexander et al. 1978; Sikka 1980 Goswami and Mohan 2001; Gadgil and Joseph 2003 etc.) into dry or wet spells of rainfall. The grouping is basically based on rainfall intensity over Indian landmass. After the onset during the end of May or first week of June, the monsoon is said to have an active phase, a break phase and a normal state. The normal state is defined by averaging the mean rainfall (or any other meteorological parameters like wind, surface pressure etc.) time series for a long duration of time and space. During the active phase the rainfall over the Indian subcontinent is much more than the predefined climatological normal. There is a widespread occurrence of rainfall over most of the Indian landmass, except over parts of Tamilnadu and parts of northeastern states. There is a formation of trough over north Indian landmass at lower level known as "monsoon trough" and another trough forms over the west coast known as "west coast trough". The position of the monsoon trough oscillates roughly between the foot hills of Himalayas to central India and is placed over central - north India during active phase. Each and every parameter like pressure, wind are seen to have distinctive characteristics features of its own which change drastically during the active or the break spells. As mentioned earlier, though, active or weak spells are defined in terms of rainfall over the central north India or the monsoon zone (Gadgil and Joseph 2003), different researchers included different parameters along with rainfall to define the active or break states. Magana and Webster (1996) defined break spells in terms of weak spells of convection and 850 hpa zonal wind speed over a large region (65^0E-95^0E, 10^0N-20^0N). Krishnan et al. (2000) defined break spell in terms of positive anomalies of outgoing longwave radiation (OLR) over the central north India. Circulation parameters are also used by many workers. Goswami and Mohan (2001) defined break spells in terms of 850 hpa wind speed at a particular grid point 15^0N, 90^0E; De et al (1998) defined in terms of cyclonic circulation, pressure and wind structures at the lower levels. The traditional rainfall intensity is also continued to be utilized to define break spells until recently (Cadet and Daniel 1988; Annamalai and Slingo 2001). Such broad classifications effectively reflect the complexity of the monsoon and it goes beyond mentioning that no single parameter can represent the situation efficiently. So the question remains the same: Can the rainfall pattern during the active or break phase be represented using only dynamical parameters in a General Circulation Model (GCM)? Or if we take that it is represented, what is the criterion to be imposed on the dynamical parameters for that? Or how accurately such states of "rain" or "no rain" are represented only with dynamical parameters even if we do not include any information of rainfall? Whether rainfall itself is the cause of active or break phase or it is the effect of such dynamical interactions?

It is evident from all the studies cited above that many parameters are required to capture the nonlinear structure of the monsoon rainfall variability. In addition to that the local and the global nature of the influence of the parameters are also important. The

influences of the circulation parameters are basically more global in nature as revealed by many earlier works which defines various indices. The circulation indices we take here are defined by Webster and Yang (1992), Goswami et al.(1999), and Wang and Fan (1999). In this paper we will try to classify the rainfall pattern from the synoptic point of view (i.e. active, break or normal states) using only the dynamical parameters and sea surface temperature (SST) without the information of rainfall and we will see how correctly the rainfall pattern is represented. It may be pointed out that the circulation indices were basically designed in the context of inter-annual variability of the monsoon system. However some recent studies (Annamalai et al., 2000 and Goswami et al. 2001) indicate that the intraseasonal and the inter-annual variability both have the common mode of spatial and temporal variability as obtained from the EOF and the Principal Component Analysis (PCA). But it is not clear till now about the skills of the large scale indices in simulating the intraseasonal variation of rainfall. It is well known from various earlier studies (e.g. Palmer and Sperber, 1996) that the large scale dynamical and the regional features are well simulated in General Circulation Models (GCM), though the models respond poorly in simulating or forecasting the rainfall. The may be due to lack of representation of sub-grid scale processes and various parameterization. Hence predicting the large scale features from the GCMs and then applying the statistical scheme for forecasting the rainfall may be a solution to the problem.

The present study is an alternate framework to describe the role of broad scale and regional scale parameters on the active and break spells which has duration of a few days to few weeks. The efficiency of the large scale dynamical forcings along with the regional parameters in defining the intraseasonal active and break pattern and assessing their role in depicting the sub-seasonal variations is being attempted in this paper. We are not interested in defining the break phase alone, as stressed by many of the earlier authors mentioned in the text. Rather, first we want to divide the rainfall pattern into discretized state in terms of many parameters taken at a time and then we will see whether the pattern match with our traditional definition of active states or break states in terms of rainfall pattern which is the key deciding factor of a dry or wet spell. The classification method used here is the Kohenen's Self Organizing Map (SOM) (Kohenen 1990; Kohenen 1995; Hewiston and Crane 2002) which falls under the class of unsupervised learning of synapses in a Artificial Neural Network algorithm. We feel that the unsupervised learning is the best option to classify the synoptic states during the monsoon season which assumes that the states are continuously evolving of its own (i.e. without any supervision) yet can be discretized into a countable number of states. Such a formulation has the following important advantages: (1) It will answer all the above questions and put forward a more efficient means of objective classification of the active and break spells using dynamical parameters.(2) It will show how the states evolving from one state to another and if the time evolution has any ordered fashion. On intraseasonal scale such information would show the evolution and movement of anomalous convection (or suppressed convection), wind patterns or any other parameters which we have chosen. (3) What are the most stable states(or nodes) and how the transient states behave during any episode? (4)How such information may be useful for developing a model dependent climatology in defining active and break state without any a-priori criterion (5) Journey towards a prediction scheme and how such information shows predictability limit?

The study may help in the following way:

- To see the role of dynamical and the thermodynamical parameters at the regional and global scale for the synoptic features associated with active or break like condition and rainfall is an effect of non-linear interactions among those parameters.

- A criteria for describing active, break and normal condition can be obtained in terms of those parameters.

- The nonlinear interactions can be described in terms of the observables in a more efficient way.

- To develop a statistical-dynamical scheme for describing Indian summer monsoon rainfall variability.

The next section will describe the SOM algorithm in brief. The subsequent sections will describe the data used, methodology developed for this study and the results.

2 Data and Methodology

2.1 Data

The dataset used for the study is the ECMWF 40 year reanalysis data (ERA-40) which is freely available for download from the ECMWF data server (http://ecmwf.int/research/).The data is downloaded from 1980 to 2001 which is used for the analysis in this paper. The daily 6 hourly global dataset for 6 months from May to September is obtained for the following parameters: u (east-west) wind (850mb and 200mb), v (north-south) wind (850mb and 200mb), geo-potential height for the 500mb, specific humidity at 850mb, precipitation, mean sea level pressure and the monthly global sea surface temperature (SST). The 6 hourly dataset for the precipitation is summed over to get the accumulated daily rainfall. The other 6 hourly parameters are averaged for the 24 hours to get the average daily value. The u-wind or the v-wind represents the large scale dynamical parameters whereas geopotential height, specific humidity and the sea-level pressure represents the local variables. The wind parameters are then converted into following large scale indices as mentioned earlier: vertical zonal wind shear index (Webster and Yang, 1992, henceforth WYI), vertical meridional wind shear index (Goswami et al. 1999, henceforth GI) and meridional shear of zonal wind index (Wang and Fan, 1999, henceforth WFI). The mean sea level pressure, geopotential height and the specific humidity are area averaged over Indian region (65^0E-95^0E, 15^0N-25^0N) to formulate the local index. The circulation indices, though originally formulated for seasonal scale, are examined first to see whether they potentially capture the intraseasonal variability. The monthly SST is taken for the regions given in Table 1. These indices are used in the SOM mapping since they found to be successfully capturing the intraseasonal variation (Fig.1).

2.2 The *Kohenen Self Organizing Map Algorithm*

The SOM algorithm developed by Kohenen as referred above usually consists of one or two dimensional neurons which are identical in nature and properties. The neurons map the less (statistically) informative input vectors to a more informative out put vector space. Thus essentially it is a clustering algorithm. Such clustering is done without any pre-information or supervision and the neurons adjust themselves according to the information provided by the data. The steps are discussed below:

(a) All the neurons of dimensionality (K1 x K2) are assigned with a initial weight vector w (i) which are random in nature with the strict condition that no two input vectors are identical.

(b) Input vectors x of dimensionality N, are broadcasted parallel to all the neurons (see fig.) and for each input vector the most responsive neuron is located. The weight vector associated with this neuron and predefined neighborhood neurons, which are assigned randomly initially, are adjusted to reduce the Euclidean distance with the input vector.

That is $\| x(n)-w_j \|$ is minimum (j=1,2,...M, & M=K1.K2).

(c) All the weight vectors are adapted accordingly as the winning neurons including those in the neighborhood are adapted. Those outside the neighborhood are kept unchanged.

$$W_j(n+1) = \begin{cases} w_j(n) + c(n)[x(n)-w_j(n)] & j \in R(n) \\ w_j(n) & \text{otherwise} \end{cases}$$

where c(n) is the adaptation constant and R(n) is the current neighborhood size centered with the winning neuron.

(d) Such steps are continued as necessary until no further change (or it reach some termination condition); the step (b) is repeated otherwise.

Thus finally the states arrange themselves according to the data. The SOM algorithm has been used for synoptic classification of states (see for example, Cavazos, 1999)). The importance of using SOM is that it assumes the data is continuous, yet the nonlinearity is well taken into account and captures the similar states. The other important advantage is that the lesser SOM nodes are allocated when the data is sparse in a region (Hewiston and Crane 2002). All these advantages prompts us to classify the synoptic states during the monsoon.

2.3 Methodology

The wind, geopotential height, specific humidity and the mean sea level pressure are used for the SOM classification of rainfall. However as mentioned earlier, both the broad scale features and the local features are found to be contributing in the evolution of the monsoon rainfall pattern. So we choose to use the daily circulation indices WYI, GI and WFI as described earlier which are based on large scale dynamical variation of wind pattern. The regional features are assumed to be represented by the daily indices defined from geopotential height, specific humidity at 850hpa and mean sea level pressure. For the actual computation of the input reference vectors of the SOM we used the standardized and smoothed anomaly values (11 day running mean) of all the indices. Henceforth all the discussion will be based on the result of using the smoothed standardized values. The non-linear combination of all the indices should sufficiently represent the complex Intraseasonal variation of the monsoon rainfall and the indices themselves have the capability of capturing the seasonality. This is shown (and justified) in fig.1 and fig.2. The influence of the Oceans on monsoon rainfall are very important from coupled ocean atmosphere interaction point of view as known from many previous works. Since the Ocean has a large memory and less day-to-day variation, we also include the monthly variation of the sea-surface temperature is also included for the classification of SOM patterns (Table-1).

The freely available software for implementing SOM is downloaded (http://www.cis.hut.fi/research/som-research/) along with detailed references and instructions for practical usage. Since it is mentioned earlier that our basic aim is to see whether the active or break like rainfall patterns can be simulated or not using dynamical parameters, we do not include the information of the precipitation during the SOM training of the nodes. The SOM classification is first made to distribute the nine (3x3) states of rainfall pattern (fig.3) with reference to central Indian region as referred in many papers for the classification of active or break phase (Cadet and Daniel 1988; Annamalai and Slingo 2001; see also Hewitson and Crane 2002; Cavazos 2000 for similar application of SOM to some other region). The choice of number of nodes is purely on physical basis since mathematically there is no restriction in choosing the resolution of the nodes. The physical justification is described in the introduction of sec. 3. The area averaged standardized rainfall anomaly is over CI for the 3x3 nodes as in Table-2. This gives a first hand impression of the most active and the most break node. The area averaged values for the selected six indices (see Table 3 for the area selection) are taken for each target day. For the same target day we have considered the data for the day itself, previous three days and forward three days. Thus we have seven days data for each of six variables (indices) i.e. 42 inputs. Along with these 42 inputs we club the monthly SST of 6 regions (given in Table-1) of Indian Ocean and the Pacific Ocean and the 1st May initial condition for each of 6 indices for a particular year. Finally the Julian day variation of each parameter is introduced as a variable according as (Cavazos 1999):

$$\sin [(2\pi t/n)-\pi/2]$$

Thus states of the corresponding dynamical pattern are obtained from 55 ((42+6) + 6+1) points spanning the dimension of the input vector (i.e. 55 coefficients for the reference vector of each node) for each day to get an output vector corresponding each node out of 2684 samples selected from 22 years of dataset. For the training purpose we have selected 2074 samples collected from 17 years and for actual classification we put 2684 samples spanning all the 22 years. The plotting of the each node illustrates how the winds, humidity and all the other parameters behave during such classified rainfall states. The nine rainfall patterns, in the fig.3 or fig.4, themselves show which is the most active or which is an intense break phase (discussed later). Next we plot the movement of the rainfall patterns 9 days (-3 triad) before the break, composite condition during the break and 9 days (+3 triad) after the break. The same thing is repeated for the active phase also. Here the break or active spells which are greater than 3 days are only plotted. The conditions of the wind or pressure or other parameters during the active or break spells are also shown and they efficiently represent all the supporting evidence of active and break spells. The mean and anomaly plots clearly show the distinction between these two rainfall states in terms of dynamical parameters (see for example, the plots of circulations at 850mb and 200mb) which are well documented in literature. We have also shown the percent probability of staying in a particular state (or node) out of all the events classified and the probability of transition from one state to other and the direction of transition. The probability of staying in a node is the probability of mapping in the same node for two consecutive occasions. The probability of transition is the probability of mapping onto the different node from a particular node. The vector for the direction of transition is obtained by picking up the relative number of transitions from one node to the other and is normalized by the total frequency of events before being plotted for direct comparison. The other important things which we show here are the seasonal trends in the rainfall events during the active and break condition and for all other classified events and the correlation of the active/break nodes with the seasonal averaged (June, July, August and September) NINO3 index, Indian Ocean Dipole (IOD) Mode index and the North Atlantic Oscillation (NAO) index. The IOD index and the NINO3 index are calculated using the SST anomalies for the prescribed region (table-1), while the NAO index is downloaded from Climate Development Centre (CDC) NOAA website. We also test our classification for three representative years: 1987, 1988 which are contrasting years of summer monsoon rainfall over Indian subcontinent and the 1997 El-Nino but normal year.

We next aim to quantify our classification of active and break states in terms of the local and global indices. For this purpose we identify the activity days for each of the nine nodes. These days for each node represent the classification to each node. Next we compute the values of each of the 6 indices for each node and the values for all the nodes are tabulated (Table-4). Then from the ERA-40 precipitation data a criteria is obtained for the days that are to be selected when the values are greater or lower than the prescribed value. A composite made from those days, thus, represents the reconstructed active or break days. The reconstructed active and the break nodes are then compared with the primary classification obtained from SOM training of the data. The composite patterns are then validated using the actual IMD precipitation data over land for the same period and from the NOAA OLR data during the same period. The inferences from the figures will be discussed in details in the next section.

3. Results and Discussion

We decide to define minimum 3x3 SOM nodes after lots of experiment and permutations. However there is no hard and fast rule in deciding the number of nodes. More the number of nodes more is the resolution and the nodes more closely represent the atmospheric continuum. The aim in choosing the said number of nodes was that at one hand it should be kept minimum and should have least distortion and sufficiently low quantization error (a measure of error due to reduction in output dimension, see S. Haykins, Ch. 9) while on the other hand it should produce maximum information of the important synoptic states discussed so far in literature (e.g. active states, break states, normal states etc.). Also from meteorological perspective the position of the monsoon trough decides the active or break-like condition over India. Now there are three positions of monsoon trough as described earlier: normal position, south of the normal position and north of the normal position. Now for each position of the trough we differentiate the states, at the sub divisional level, into normal, below normal and above normal cases, which gives a total of 9 states. We feel that the assumption is justified since the attention in literature is given to 3 basic states: active, break or normal states. The inclusion of three more transition states for each of the above states is required to have a more detailed idea of regional patterns and about its movement from one phase to the other. If we resolve more states, though the error gradually decreases, the states of monsoon are not distinguishable from each other and also involves more computer work-time. So considering a mathematical optimization and meteorological perspective, 3x3 states is chosen. The states sufficiently represent the active break states and transitions. This can be seen in Table-2. We produce the area averaged rainfall values over CI for each node in Table -2. The values show that the states having negative values of area averaged standardized anomaly of rainfall can be termed as acute break state (1, 3), less acute break states [(2, 3) and (3, 3)], normal to the negative side (1, 2), normal to the positive sides(3,2), less intense active states [(2,1) and (3,2)]and intense active states (3,1) and a complete neutral state(2,2). The complete neutral state has a near zero value of rainfall anomaly compared to all other state. Such states are also showing transition when we compare rainfall anomalies.

The sub sections below will describe the details of results obtained using such classification. The application of SOM classification removes the ambiguity or confusion that may creep up while classifying rainfall events in a synoptic way: whether or not a state can be said an active state or a break state or a normal state which so far actually depends on the experience of the observer.

3.1 *The representation of monsoon rainfall in terms of the indices of dynamical parameters:*

It is mentioned elsewhere that the robustness of the large scale and the regional parameters that are used in the intraseasonal classification of SOM nodes has to be discussed first to be sure of their application in the sub-seasonal classification. The fig.1 shows the area averaged (15^0N-25^0N, 70^0E-85^0E) seasonal mean of all of the indices plotted along with the precipitation data obtained from the ERA-40 and the actual ground based observation obtained from the India Met. Dept. for the same period (1980-2001).

The shaded region in all the plots shows the variation within the ±1 standard deviation range. It can be seen that all the indices have the similar intraseasonal variation as that of the precipitation. The Wang and Fan index seems to have a more detectable intraseasonal pattern. The variation in rainfall pattern is more amplified in this index. The other broad scale indices are also capturing the basic Gaussian structure of the intraseasonal rainfall pattern. The fig.2(a) shows the intraseasonal variability of all the indices along with the rainfall pattern. The figure is shown for the year 1987 and 1988 for the sake of clarification in the two contrasting monsoon years. The figure 2(b) shows the plot of the area averaged value of rainfall anomalies over CI and the area averaged value of rainfall composite for each class for a particular day in year 1987 and 1988 which are mapped onto the SOM nodes (Table-2). The strong fluctuations (though in a very complex manner) of all the indices in fig 2(a) in the intraseasonal scale and the density of classes in the positive (negative) side in the year 1988(1987) shows that a judicious selection of large scale and regional scale indices may describe the intraseasonal rainfall pattern.

3.1(a) Classification of Precipitation States

The application of SOM technique is justified only if we can reproduce the synoptic classification of rainfall pattern. The fig.3 shows the 3x3=9 states of the anomalous rainfall pattern which is produced using the dynamical parameters described in section 2.1. It is clear that the corners (1, 3) and (3,1) shows the patterns of break and active condition respectively and they are easily distinguishable without the use of rainfall data. From now onwards the state (3, 1) will be termed as active (or wettest) state and the state (1, 3) as a break (or driest) state. The active and break states are taken with reference to central India (15^0-25^0N, 70^0-85^0E, henceforth CI) where a prominent precipitation extremum has an important contribution in the seasonal mean rainfall value. During the active phase (3, 1) the mean precipitation is maximum over central India and suppressed over northeastern states and Tamilnadu (east) coast in the peninsular India. The condition is reversed in the state (1, 3) where there is a rainfall maximum over northeastern states and Tamilnadu coast and has a minimum over the rest of Indian subcontinent. It also clearly shows a phase reversal in the eastern coast and the northeastern states during active and break states. The other states in the figures 3 are states showing transition from one state to the other. The states (1,1) or (2,1) (fig.3), we take as an example, also shows high positive rainfall anomalies but most of the rainfall is towards the lower part of the peninsula or over the ocean and hence it can not be termed as a break or active phase over CI. The corresponding states of circulation and other local indices like MSLP, specific humidity and geopotential height also shows the systematic transition as seen from precipitation anomaly (fig.3). The SOM patterns for all the other dynamical parameters are described through fig.4 to fig. 10.The anomalous MSLP (fig. 8) and the geopotential height (GPH) (fig.9) shows that for the most active state (3, 1) the closed iso-lines (or low pressure center) are broadly spread over central north India and over the Arabian Sea and Bay of Bengal. Though the convection centers in fig. 3 are also intense and organized in (2, 1) and (1, 1), they are mostly over ocean and peninsular part of India whereas central and northern parts depicts less rainfall in those states. Similarly the states (2, 3) and (3, 3) represents the break-like condition and the state (3,1) being the intense break state as discussed earlier. Similarly for the states (2, 3) and (3, 3) global and

the local dynamical features as represented by circulations, geopotential height, specific humidity and mean sea level pressure can also be seen to represent the break like condition for the same states of precipitation. In the state (3, 3) there is a development of negative pressure anomalies, though the gradient is not seen to be strong. The state (3, 2) however shows more pressure gradient fields which has the effect of increased rainfall anomaly for the same node as can be seen from the precipitation anomaly. An interesting observation can be made from the comparison of all the anomalies e.g. MSLP (fig.8), GPH (fig. 9) and the specific humidity (sph) at 850 level (fig. 10) with the precipation anomaly (fig.3): that for some of the nodes (e.g. 1, 1) there is a mismatch between rainfall pattern and the parameter(i.e. MSLP and GPH) pattern. It may be noted that there is a development of week positive pressure anomalies at node (1, 1), though positive precipitation pattern remains persisted (though weak over land).This shows a time lag between a variation in the rainfall and pressure pattern. However for other parameter like sph, the pattern match with rainfall at the same node (1, 1) i.e. there is a high rainfall when there is an ample supply of moisture; thus showing no lag. So rainfall indeed is a complex interaction between all the parameters. The states (1, 2), (2, 2) and (3, 2) is seen to be intermediate of all the states for precipitation hence we call them normal states and as we will see later, a random transition may take place to any state. During the active stage (3, 1), the ITCZ (as represented by the precipitation band) is active over whole of the continent and extends up to pacific. There is also a signal of developing suppressed convection anomalies in the equatorial Indian Ocean. This anomaly is seen to be moving northward (the direction of movement as will be discussed little later.

3.1(b) Classification of large scale circulation patterns

The detailed features anomalous 850mb wind streamline and vorticity are plotted in fig.4 respectively and anomalous wind vector and magnitude in fig. 5 respectively. The anomalous wind states are actually showing nicely the characteristics features of circulations during the break state and the active state (state (1,3) and state(3,1)) as can be seen in literature (Goswami and Mohan 2001, Gadgil and Joseph 2003). The strength of magnitude of wind vectors are increased significantly during active state and are reduced during the break state. The plots in figures, as mentioned above, show the time evolution of the increment or decrement of magnitude. It can be seen in the figure 6 that during the active (break) phase strong (weak) westerlies over the Indian region and the anomalous wind showing westerlies during active phase and easterlies during the break phase. The wind vectors in fig.5 also show anomalous anticyclonic winds over Indian Ocean during active phase and cyclonic circulation during the break phase. The streamlines (fig. 4) are also showing close packing during the active phase over the Indian region and the curvature across the monsoon trough can also be seen. The break state in the same figure also clearly shows less packing of the streamline and the absence of monsoon trough leads to less pronounced curvature. The lower level large positive vorticity can also be seen in active state which is absent during the break state (actually negative over western India). The anomaly vorticity and the streamlines are actually opposite in nature which can be seen from fig.4 during the active and the break condition only to support the mean wind conditions shown in the previous figure. The wind patterns in the other nodes show a transition pattern from or towards active or break states.

The circulation features at the 200mb are plotted in figs.6 and 7. The mean wind shows Tibetan anticyclone is extended to the west of its normal position and is widespread over the subcontinent (fig. not shown). The anomalous vorticity also shows a shifting of the positive core towards west during the break phase than the active phase The break phase shows the circulation is towards the east of its normal position (the normal phase may be the state (1,1) (2,2) or (3,3) as confirmed from precipitation states in fig. 4. The strong easterlies (Tropical Easterly Jet) over the Indian subcontinent can be seen during the active phase below 15^0N over a larger region as compared to the break state in fig. 7. The westerly jet stream are much strong during the break state than the active state and the anomalous wind (Fig.7) is showing the extension of the core below 40^0N during the break phase than in the active phase in which the strength is considerably reduced.. The actual plot of u and v wind is comparable to the earlier description (figs. not shown). The mean u wind shows strong easterly jet at 200mb during active phase. During the active phase there is a large anomalous v wind from the Indian landmass showing the return circulation of the anomalous Hadley cell that develops over Indian subcontinent.

3.1(c) Classification of regional dynamical patterns

The detailed features of mean sea level pressure (MSLP) are examined next. The trough over the CI is clear from the mean plot which is seen to be shifted towards foothills of Himalayas during the break phase (figs. not shown). This is also clear from anomaly plot (fig. 8) which shows negative pressure anomaly over whole India during active phase and positive pressure anomaly during the break phase. Also the number of isobars over India is seen to be much more during the active phase than the break phase. The anomalous 500mb geopotential height is also plotted in fig.9 to support the surface observations. The anomalous specific humidity at 850mb is also plotted in figure 10 to show the spatial and temporal distribution of available water content. The mean plot shows the high perceptible water during the active phase over the CI region than the break phase where it is shifted towards the northeastern parts of India (fig. not shown). The anomaly pattern depicts positive values during active state or negative values during the break phase (with slight positive values near foothills).

The above discussions show conclusively the patterns of dynamical parameters can efficiently simulate the rainfall pattern during the monsoon season and those patterns are representative of active or break (or normal) states. The requirements of all these seven parameters shows the rainfall is the effect of many interactions, though nonlinear, can be classified logically using the SOM algorithm. It is worth mentioning here that all the states are showing some features discretized from others and some states give good rainfalls than other. So in true sense many states are giving rainfall over many parts and many states don't give rainfall which can cause drought over some parts of India and flood to the other part.

3.2. Stability of the states and the direction of movement

In the last section we have talked about the time evolution of the states. The direction of evolution will give the important information of the temporal movement and its variability. This is plotted in fig.11 (a).The figure clearly shows that the direction of movement is mostly in a clockwise in sense. Some states shows probability of transition to a particular direction only while the other state shows movement to any of the nearby available state. For example, the state (1,3) shows absolute probability of transition to the state (2,3) while the state (2,2) shows the probability of transition to any of the nearest neighborhood. This figure is a clear indication of the uncertainty of transition in a particular direction. It actually shows some states are more predictable than others. If the system is in state (1,3) we can certainly say that the next transition state will be (2,3) while if it happened to be in state (2,2) it is most unpredictable. Similarly the break state (3,1) shows almost certainly that the next transition state to be (2,3). Thus transition from active or break state are more directed to a particular state while the other states are more "confused". This may explain the reason of failure of the model at times. The inherent uncertainty of an integration state may lead to a wrong state in next step of integration. The cause of this uncertainty may arise from the degree of non linearity associated with a state because some states have more "degrees of freedom" than the others which is inherent with a nonlinear system. This in simple sense implies that if the system is in an active state, will definitely move towards a less active state and the same conclusion are also valid for a break state. If the system is in an intermediate state it has a comparative probability (high confusion) of all nearest neighbors. Thus we can infer that the low entropy (more informative) corner states are more predictable for transition to the other states.

The stability at each node (probability of no transition) is also important beside the probability of transition. The probality of staying in a particular state is plotted in fig.11(c). The figures in each box shows the percentage probablity of staying in that state once the system has arrived at that node. It is very clear that active state and the break state are the more stable states than others. The states (1,1) and (3,3) are also somewhat stable than remaining 5 states. However the indication is clear from the figure that the active or break states are more stable states. Thus if we concern only on intense break states and probablity of transition from that state we can say that once the system is in an intense break or active condition, it has the strong affinity of staying in that state rather than transition. The state is in some sort of dynamic equillibrium. This may explain why the atmospheric conditions sometimes lead to an unusual break spell of prolonged duration. Once all the dynamical parameters have the condition of state (1, 3) (tobe discussed later), it will lead to a prolonged break. However the advantage of finding a system in such a state is that the predictability of transitions is also increased from those states!

The percentage frequency of staying at each node per year is plotted in fig. 11(d). This shows the average frequency of staying in the active node or the break node is highest and is equal (21). The next plot fig.11 (e) shows the mean days per event in a season. The most active and the most break nodes are showing that the mean number of days of staying in those states is more than other states. This actually supports the high probability of staying during the active state or break state as plotted in earlier figure.

3.3 Movement of Precipitation bands during the active or break phase over Central India

The last subsection describes the movement of the systems as a whole from the sample obtained in a SOM node. We also wish to check whether the composite behavior of the movement can be seen by plotting a triad or not. For this purpose we classify the active and the break days for each year and made a composite of the entire active and the break phase. The composite is made for the active or break nodes from the days identified in that node using SOM. The triad value of the composite of breaks/actives greater than three days is plotted from three triads before the break/active phase to the three triad after the break/active phase. The triad 0- (0+) depicts the state when the system entered (left) the break/active stage. The middle state (all composite) is the composite of all the break or active state.

The movement of the break phase (state (1, 3)) (fig.12) structure shows that the movement started from triad -3, and ended at triad +3, both of which are more or less normal states. The negative precipitation anomaly started from Indian Ocean bifurcated to Bay of Bengal and Arabian Sea and finally arrived to land at triad 0-. At the composite structure the equatorial Indian Ocean shows the signal of increased convection which subsequently moves northward towards the subcontinent in the succeeding triads.

The movement of the precipitation band during the active phase (state (3, 1)) is seen clearly starting from the Indian Ocean in fig. 13. The precipitation band is well established over Indian land mass in the triad 0-, all composite, and 0+. On and after the triad +1 the negative precipitation anomaly starts propagating from the Bay of Bengal. Such propagation may be seen as a Rossby wave response as described by many authors (Krishnan et al., 2000; Annamalai and Sperber, 2005).

3.4 The correlation of the SOM nodes with ENSO, IOD and NAO

The events like ENSO, IOD and the NAO are referred to as significant factors determining the intensity, spatial and the temporal variability of the monsoon. The seasonal averaged ENSO index, IOD index and the NAO index, which are determined as mentioned elsewhere, is used to correlate with the activity days obtained from SOM classification from 22 years of data for each node. Thus for the most active node (3,1) it gives a day-to-day correlation of the dates in the active spells greater than 3 days in a season with the values of ENSO index for the same dates. The correlation coefficients are plotted in fig.14. An examination of figures for each node for ENSO index shows that the break state (1,3) is highly correlated with ENSO at a 99% level of confidence, the states (3,2) and (2,3) are correlated at 5% level of significance, while no other states including the intense active state (3,1) are not at all significantly correlated. Thus the role of ENSO with the acute break phases of Indian summer monsoon can be associated in a qualitative way. The other two indexes like IOD index or the NAO index, however, are seen not to be significantly correlated with any nodes.

3.5 The Trends in the Rainfall pattern and some case studies

The seasonal averaged trends in the rainfall pattern are plotted in fig.11(b).The figure clearly shows that the states (2,3), (3,3) and (3,2) shows higher increasing trend while the states (1,1), (1,2) and (3,1) shows the increasing trend and the state (1,2) is significant at 2% level. The state (1,2) represents an intense break like situation in peninsular India.This supports the important notion that the extreme states or weather conditions are going to prevail replacing the normal states which is the conclusion of many recent climate change experiments (see for example Rupakumar et al 2006). The role of Green House gases, though, can't be assessed directly from the study done here, it can be said that the role of initial conditions and continuous existence of extreme events due to climate change in a sample can have a significant role in determining the trend.

Finally the case study for the year 1987, 1988,1994 and 1997 are shown in fig. 15 to substantiate the effectiveness of SOM algorithm for year wise study. The year 1987 is a drought year, 1988 is a flood year and 1997 is a normal year. The figures for the year 1987 shows that there are 73 acute break days (state (1, 3)) and only 15 intense active days (state (3,1)), and the year 1988 shows that there are 32 active days and 3 break days. Thus the opposite conditions are nicely captured in the figure. The year 1994 is an IOD and good monsoon year. It can be seen that the number of active days are more in the most active node (3,1). The year 1997 shows comparative numbers of active and break phases though the number of break phases are more, while the other number of other phases decreased considerably. An interesting observation can be made from these figures and the correlation coefficient values projected for each node in fig.14. The figures of correlation indicate that only break days is significantly correlated, which means that in an El Nino year number of breaks should be more than non El Nino years, while, the active phase is related insignificantly with the ENSO phenomena. This leaves the impression that the dynamics of active and break states are separately related to ENSO phenomena hence ENSO index may not be a good indicator of active or normal monsoon year.

3.6 The quantification of the active and break states

We have discussed earlier about the states (3, 1) and (1, 3) which are classified as the most active and break states of rainfall pattern. The dynamical features corresponding to those states clearly support the rainfall states. However, as is our aim, it is important to quantify those classifications. Such quantification is achieved by computing the values of the indices (like WYI, GI etc.) for each of 9 SOM nodes which are used in SOM classification. The standardized anomaly values of the indices are given in Table -4. The result indicates that for the most active (3,1) and the break node (1,3) all the values are close to ±1 with the exception of Wang and Fan index. The value of ±1 is a statistically sound criterion. Thus to see the role of the regional and the global parameters and at the same time assuming a stringent statistical criteria for the most vigorous period of monsoon fluctuation, i.e., during 15th June to 15th September, the standardized anomaly values for the states (3, 1) and (1, 3) are taken to be ±1 and is given in Table -3. A careful observation shows that the values of the indices are just opposite in nature as the SOM

nodes are mapped in figure. The days are obtained next from the 22 years dataset when the values of the parameters are greater or less than the prescribe value to represent the active or break like situation. A reconstruction of the states using the same days and the condition described in Table-3 from the NOAA OLR data for the same period (1980-2001) shows similar spatial features of active and breaks states (fig. 16). The reconstruction shows a close resemblance with SOM node. It also captured all the basic global features of active and break phases as discussed in various literatures (e.g. Gadgil and Joseph, 2003) as obtained in the primary classification (fig.4). However it is important to note that though the gross spatial features are nearly opposite using the opposite values of the indices for the active and break states, they are not exactly opposite. Thus the dynamical forcings governing the arrival of active and break states may not be exactly opposite in nature or may not be equally tuned to contrasting characters of active or break phase. For the Indian landmass we have compared the SOM reconstructed ERA-40 rainfall with the IMD rainfall data over land for the same period (1980-2001). The reconstruction using the rainfall is obtained for the whole globe (figs. not shown). However for the sake of comparison and validation the spatial distribution of the rainfall pattern during the active and break phase is given in figs. 17 and 18. The top panels show the ERA-40 active or break states and the bottom panels show the active or break condition for the IMD 1^0X1^0 data. It can be easily verified that the rainfall map using the SOM criteria proposed in Table-3 and the days identified for active and break phases from the ERA-40 data captured all the basic features of rainfall during the active or break phase from IMD rainfall data as described by various other studies (Gadgil and Joseph, 2003) and is also comparable with ERA-40 reconstruction.

4. Conclusion

We briefly summarize below the results of the study:

1. The SOM algorithm can be used as an excellent tool to describe and classify the states of Indian Summer Monsoon. The synoptic classifications of active and break states are easily achieved using the SOM technique. The states are classified as active state, break state, normal state and the transition states. The 3x3 mapping shows 3 active states (with state (3,1) being intense active state), 3 normal states and the 3 break states (with state (1,3) being an acute break state).

2. It is possible to achieve the perfect classification of states only with dynamical parameters like wind, MSLP, specific humidity etc. without the information of rainfall. There are three global and three local indices used in the classification. They are vertical zonal wind shear index (WYI), vertical meridional wind shear index (GI) and meridional shear of zonal wind index (WFI). The mean sea level pressure, geopotential height and the specific humidity are area averaged over the region (65^0E-95^0E, 15^0N-25^0N) to formulate local indices. These indices themselves show intraseasonal variation and can be seen to describe the active and break patterns of rainfall. Hence the role of global and the local parameters represented by the indices are evident in this study.

3. Most of the dynamical models are able to capture large scale spatial and temporal variation of the dynamical parameters realistically (Sperber and Palmer, 1996) but the simulation of rainfall is very poor. This discrepancy may be attributed to poor physical parameterization. Therefore this study can be extended to obtain realistic rainfall simulation by developing statistical relationship with dynamical parameters simulated by the GCMs and rainfall.

4. The active and break nodes show good probability of transition to a single nearest neighbor with less ambiguity. The probability of staying in active or break states is also more than that of the intermediate states and the normal states. The ambiguous probability of transition may be due to non linear interactions among various parameters. The percentage frequency of staying in a particular node per year is maximum at the active and break node.

5. The study can be used to quantify the values of dynamical parameters during the active and break states. Such quantification may be used to estimate actual value of the rainfall at each node which we wish to show in a future study.

6. The SOM derived active and break state composite triads nicely show the northward propagation of the rainfall band. The suppressed convection anomaly can also be seen propagating northward during the initiation of the break phase.

7. The correlation analysis shows that only break phase (seasonal total of number of break days) is significantly correlated to the seasonal ENSO index (the active phase is mildly correlated without significance). The IOD index and NAO index are also insignificantly correlated.

8. The year wise study illustrates that active and break nodes are correctly observed each year. It also indicates the dynamics of active and break phase are differently related to ENSO, the relation with break state being statistically significant.

9. The trend in the rainfall pattern shows increasing trend of extreme states and decreasing trend of normal states. Such trends are already predicted by climate change experiments incorporating the effect of Green House effect.

10. A scientifically satisfying quantification of active and break state can be achieved using the values of six indices. Though active and break states have opposite values of indices the states are not exactly opposite in spatial distribution of rainfall pattern. This may be due to the fact that the dynamical forcings governing the arrival of active and break states may not be exactly opposite in nature or may not be equally tuned to contrasting characters of active or break phase.

11. A reconstruction of active and break states using the prescribed values of indices (as in Table -3) capture very nicely the features of active and break states as obtained from primary classification. The reconstruction is also verified using the IMD rainfall data over land for the same period. The composite features of active and break states are well captured even if the days are identified using ERA-40 data.

Acknowledgements

We are thankful to the Director, Indian Institute of Tropical Meteorology, Pune, India for his constant encouragement. We are also thankful to Dr. R. Krishnan for discussions and valuable suggestions. The financial support from the Department of Ocean Development, Govt. of India, under the project 'Air-sea interaction in the Indian Ocean region' is also acknowledged.

Table-1

The six regions over which SST is used in SOM classification.

50E-70E	90E-110E	150E-180E	180E-210E	210E-270E	110E-140E
10S-10N	10S-0N	15S-5N	5S-5N	5S-5N	0N-20N

Table-2

Values of area averaged standardized anomalies of rainfall from ERA-40 data over central India for all 3x3 SOM nodes.

(1,3) -2.04	(2,3) -1.23	(3,3) -0.54
(1,2) -0.60	(2,2) 0.03	(3,2) 0.37
(1,1) 0.41	(2,1) 0.85	(3,1) 2.39

Table- 3

Table showing the objective criteria that should be satisfied for at least three continuous days(or more) by different indices for determining active(break) days.

Index (all values in standardized anomalies)	***Active State***	***Break State***
Either		
Goswami et al. Index V850(70^0-110^0E,10^0S-30^0N) – V200(70^0-110^0E,10^0S-30^0N)	>1	< -1
or		
Wang and Fang Index U850(40^0-80^0E,5^0N-15^0N) - U850(60^0-90^0E,20^0-30^0N)	>1	< -1
or		
Webster and Yang Index U850(40^0-110^0E,0^0-20^0N) – U200(40^0-110^0E,0^0-20^0N)	>1	< -1
And		
Either		
Mean sea level pressure index (65^0E-95^0E,15^0N-25^0N)	<-1	> 1
or		
Specific humidity (850mb) index (65^0E-95^0E,15^0N-25^0N)	>1	<-1
or		
Geopotential Height (500mb) Index(65^0E-95^0E,10^0N-20^0N)	<-1	>1

Table-4

Values of area averaged standardized anomalies of different indices from ERA-40 data over central India for all 3x3 SOM nodes

Webster Wind index

-1.00	0.11	0.61
-0.51	0.26	0.83
-0.04	0.26	0.74

Goswami wind index

-0.67	-0.41	-0.05
-0.34	-0.05	0.26
0.24	0.51	0.70

Wang wind index

-0.94	-0.49	-0.04
-0.26	0.08	0.35
-0.03	0.37	1.14

Geopotential height index

0.81	-0.02	-0.81
0.60	0.13	-0.66
0.50	-0.03	-0.84

Specific humidity 850hpa index

-0.91	-0.74	-0.71
0.07	0.01	0.03
0.67	0.72	1.09

MSLP index

1.02	0.32	-0.48
0.64	0.04	-0.71
0.26	-0.28	-1.12

References

Alexander, G., R. N. Keshavamurthy, U. S. De, R. Chellappa, S. K. Das, and P. V. Pillai, Fluctuations of monsoon activity, Indian J. Meteor. Geophys, 29, 76-87, 1978.

Annamalai, H.,and J. Slingo, Active/break cycles:diagnosis of the intraseasonal variability of the Asian Summer Monsoon, *Clim. Dyn*.,18, 85-102, 2001.

Annamalai, H., and K. R. Sperber, Regional heat sources and the active and break phases of boreal summer intraseasonal (30-50 day) variability. *J.Atmos.Sci*.,62, 2726-2745, 2005.

Blanford, H.F., Rainfall of India; *Mem. Ind. Met. Dept*.,2, 217-448,1886.

Cadet, K. L., and P. Daniel, Long–range forecast of the break and the active summer monsoons, *Tellus*, 40, 133-150, 1988.

Cavazos, T., Large scale circulation anomalies conducive to extreme precipitation events and derivation of daily rainfall in northern eastern Mexico and southeastern Texas, *J. Climate*, 12, 1506-1523, 1999.

Goswami, B. N. and R. S. A. Mohan, Intraseasonal Oscillations and Interannual variability of Indian summer monsoon, J. Climate, 14, 1180-1198, 2000.

Gadgil., S. and P. V. Joseph, On breaks of Indian summer Monsoon, *Proc. Indian Acad. Sci. (Earth Planet Sci.),* 112, 529-558,2003.

Goswami, B. N., V. Krishnamurthy, H. Annamalai, A broad scale circulation index for the interannual variability of the Indian summer monsoon. *QJRMS*. 125:611-633, 1999.

Hewitson, B.C., and R. G. Crane, Self organizing maps: application to synoptic climatology. *Climate research*.22:13-26, 2002.

Kohenen, T., The self organizing map. *Proc IEEE .78(9):*1464-1480.1990.

Krishnan, R., C. Zhang and M. Suji (2000) Dynamics of breaks in the Indian Summer Monsoon. J. Atm. Sci.57:1354-1372.

Krishnamurthy, T., and H. N. Bhalme, Oscillations of a monsoon system. Part 1. Observational aspects, *J. Atmos. Sci.*, 33, 1937-1954, 1976.

Malurkar, S. L., Notes on analysis of weather of India and neighbourhood, Memoirs of I. Met. D. XXVII Part IV,139-215,1950.

Magana, V., and P. J. Webster, Atmospheric circulations during the active and break periods of the Asian summer monsoon; Preprints of the Eighth Conference on the Global Ocean-Atmosphere-Land System(GOALS); *Amer. Meteorol. Soc*, Atlanta, GA,1996.

Raghavan, K., Break monsoon over India, *Mon. Wea. Rev*., 101, 33-43, 1973.

Rajeevan, M., J. Bhate, J. D. Kale and B. Lal, A high resolution daily gridded rainfall for the Indian region: analysis of active and break monsoon spells, *Curr. Sci*. 2006 (In press).

Ramamurthy, K., Monsoon of India: Some aspects of the break in the Indian southwest monsoon during July and August, *Forcasting Manual No. IV 18.3; India Met. Dept., Poona, India*, 1-57, 1969.

K. Rupa Kumar, A. K. Sahai, K. Krishna Kumar, S. K. Patwardhan, P. K. Mishra, J. V. Revadekar, K. Kamala and G. B. Pant, High-resolution climate change scenarios for India for the 21st century,90, *Curr. Sci*, 334, 2006.

Sikka, D. R., Some aspects of the large scale fluctuations of summer monsoon rainfall over India in relation to fluctuations in the planetary and regional scale circulation parameters, *Proc. Indian Acad. Sci. (Earth Planet Sci.)*, 89, 179-195,1980.

Sperber, K. R., J. M. Slingo and H. Annamalai, Predictability and the relationship between subseasonal and interannual variability during the Asian summer monsoon. *QJRMS*, 126, 2545-2574, 2000.

Wang B and Fan Z. Choice of South Asian summer monsoon indices, *Bulletin of the American Meteorological Society*. 80:629-638, 1999.

Webster, P. J. and S. Yang, Monsoon and ENSO: selectively interactive systems. *QJRMS*. 118:877-926, 1992.

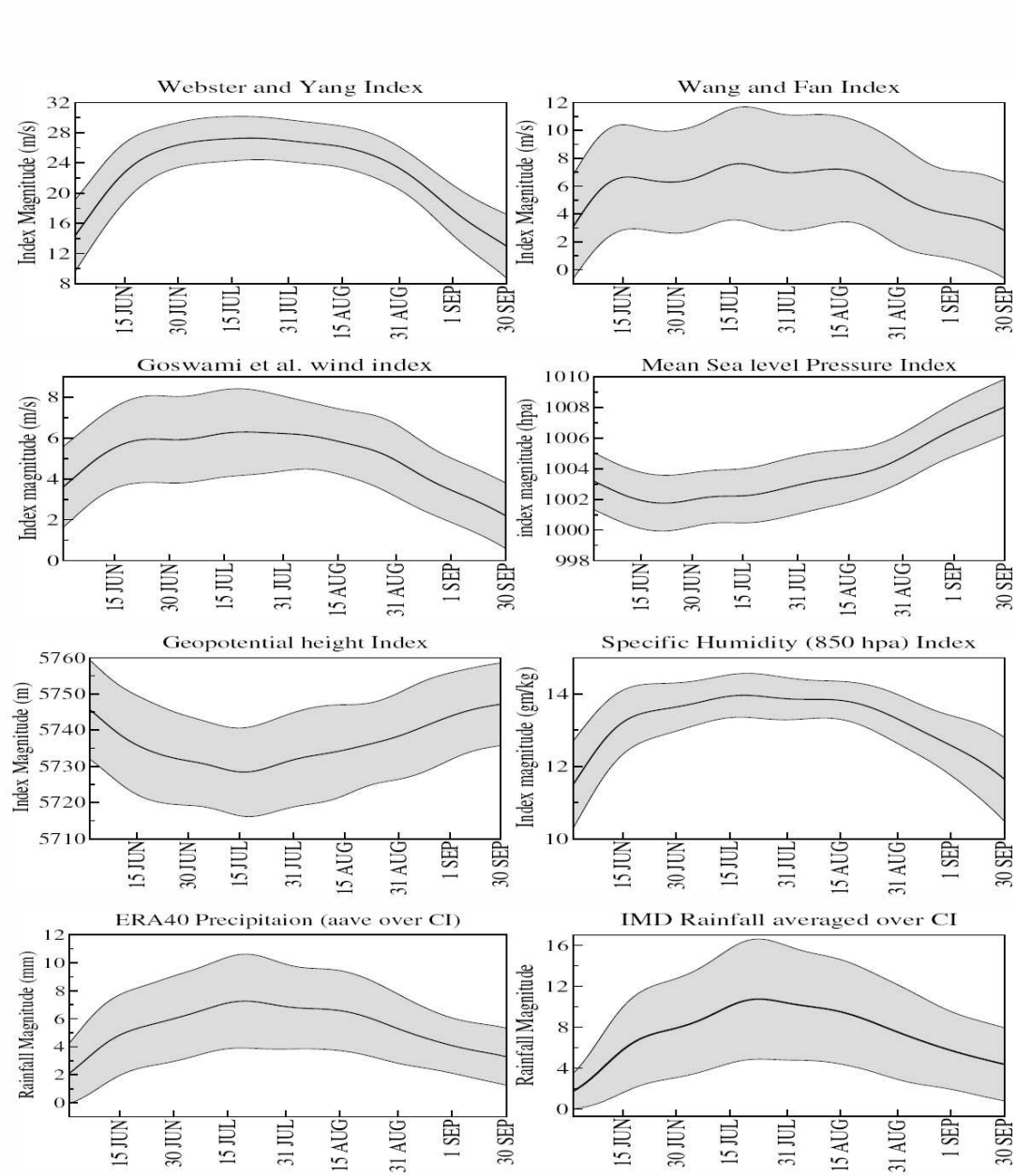

Figure 1 : Plot showing the 22 year climatological daily mean (1 June to 30 Sep) of all the indices. The shaded region shows the values with one standard deviation above and below normal.

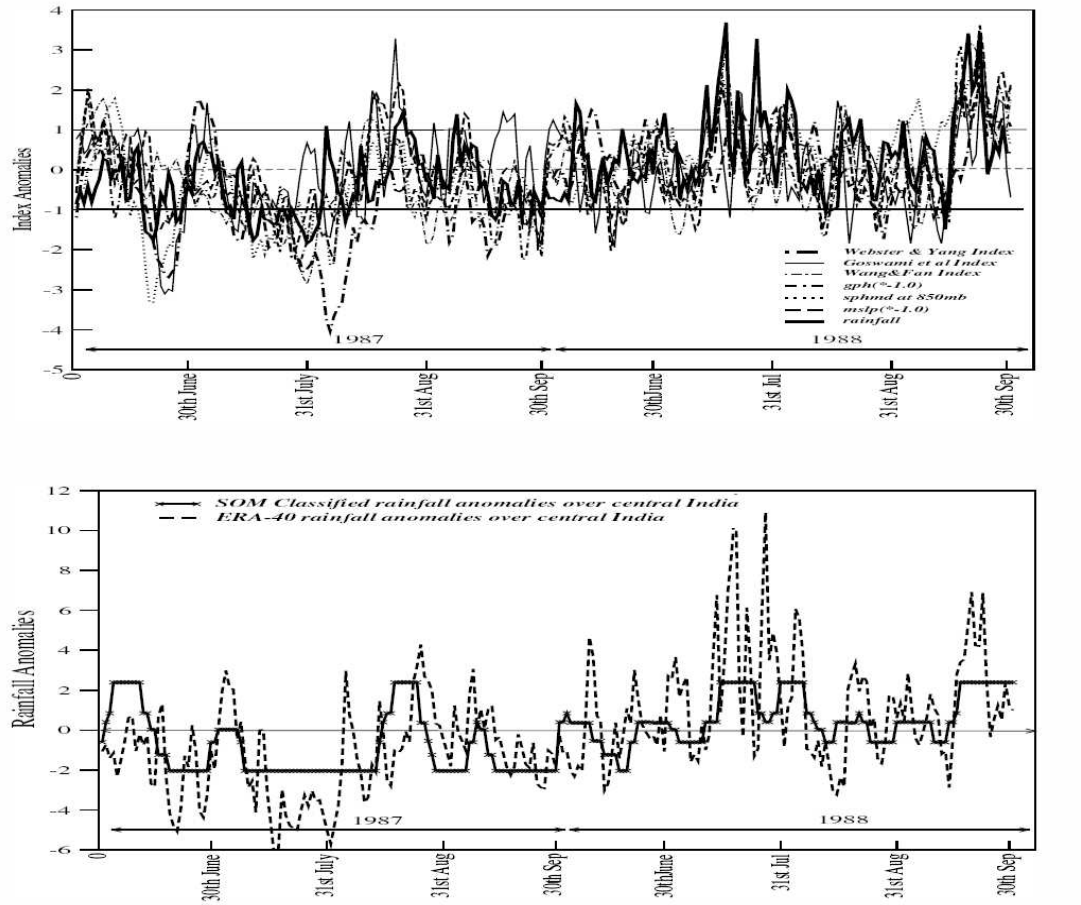

Figure 2: (a)The plot shows the intraseasonal oscillation of all the indices during the year 1987 and 1988. The MSLP and the GPH are multiplied by -1.0 to revert the phase of the two indices.(b) The plot showing the efficiency in capturing the rainfall pattern by SOM.The thick line show the area averaged rainfall anomaly composite for the 3x3 SOM class for the period 1980-2001. The broken curve show the area averaged rainfall anomaly from Jun to Sept. for the year 1987 to 1988.

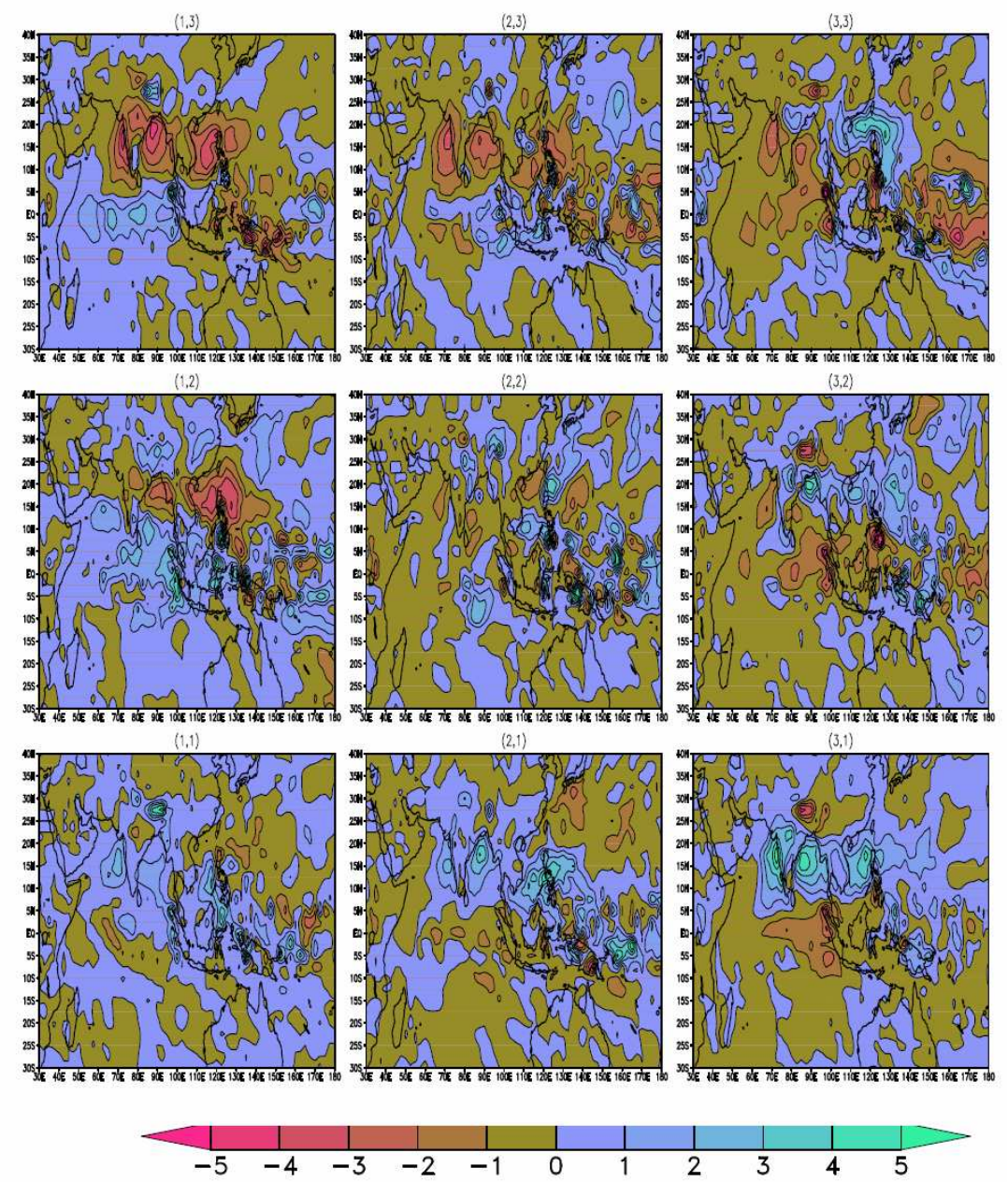

Figure 3: The plot shows the anomalous precipitation states for SOM classified pattern. The values of each 3x3 node are the composite anomaly of all the days classified in that node. The states show the wettest(active) node is (3,1) and the driest (break)node is (1,3)(units mm/day).

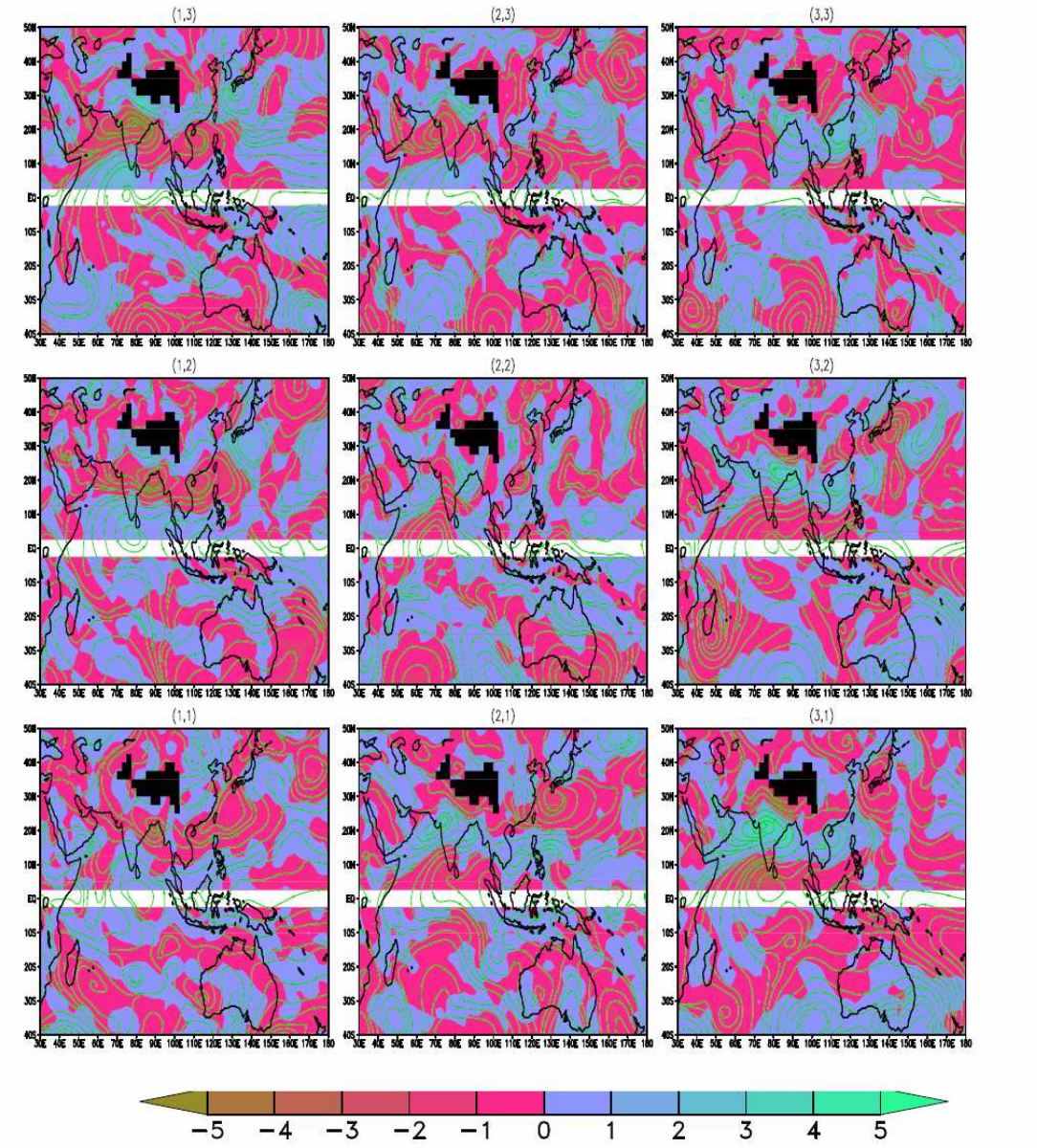

Figure 4: The plot is same as fig.3 but showing the 850hpa anomalous wind streamline and vorticity(shaded). The values of each 3x3 node are the composite anomaly of all the days classified in that node.The values above 2000m is masked over Tibet. (units 10**-5/sec)

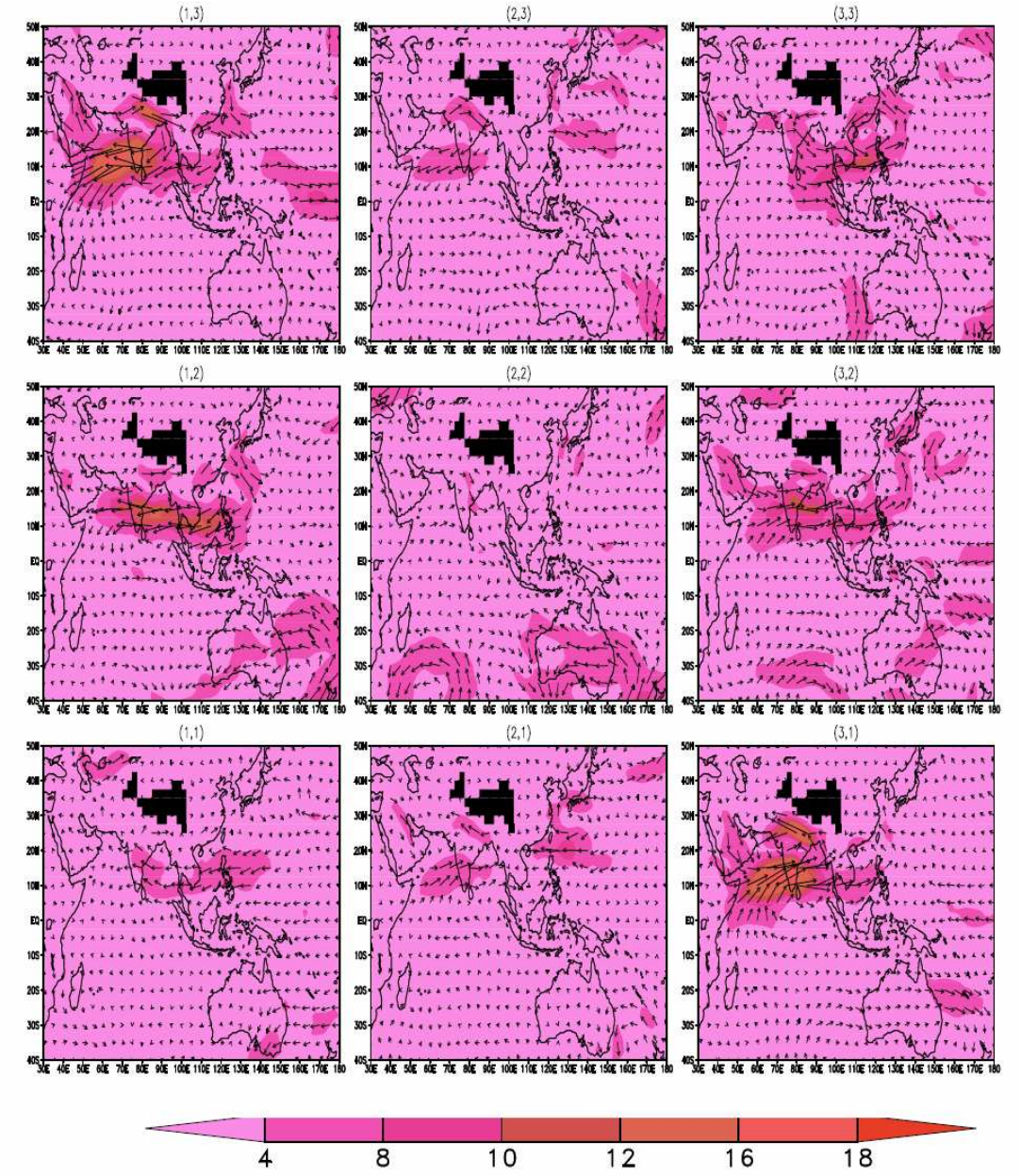

Figure 5: The plot of 850hpa wind showing anomalous vector and magnitude (shaded) for all SOM nodes.The values of each 3x3 node are the composite anomaly of all the days classified in that node.The values above 2000m is masked over Tibet.(units m/sec)

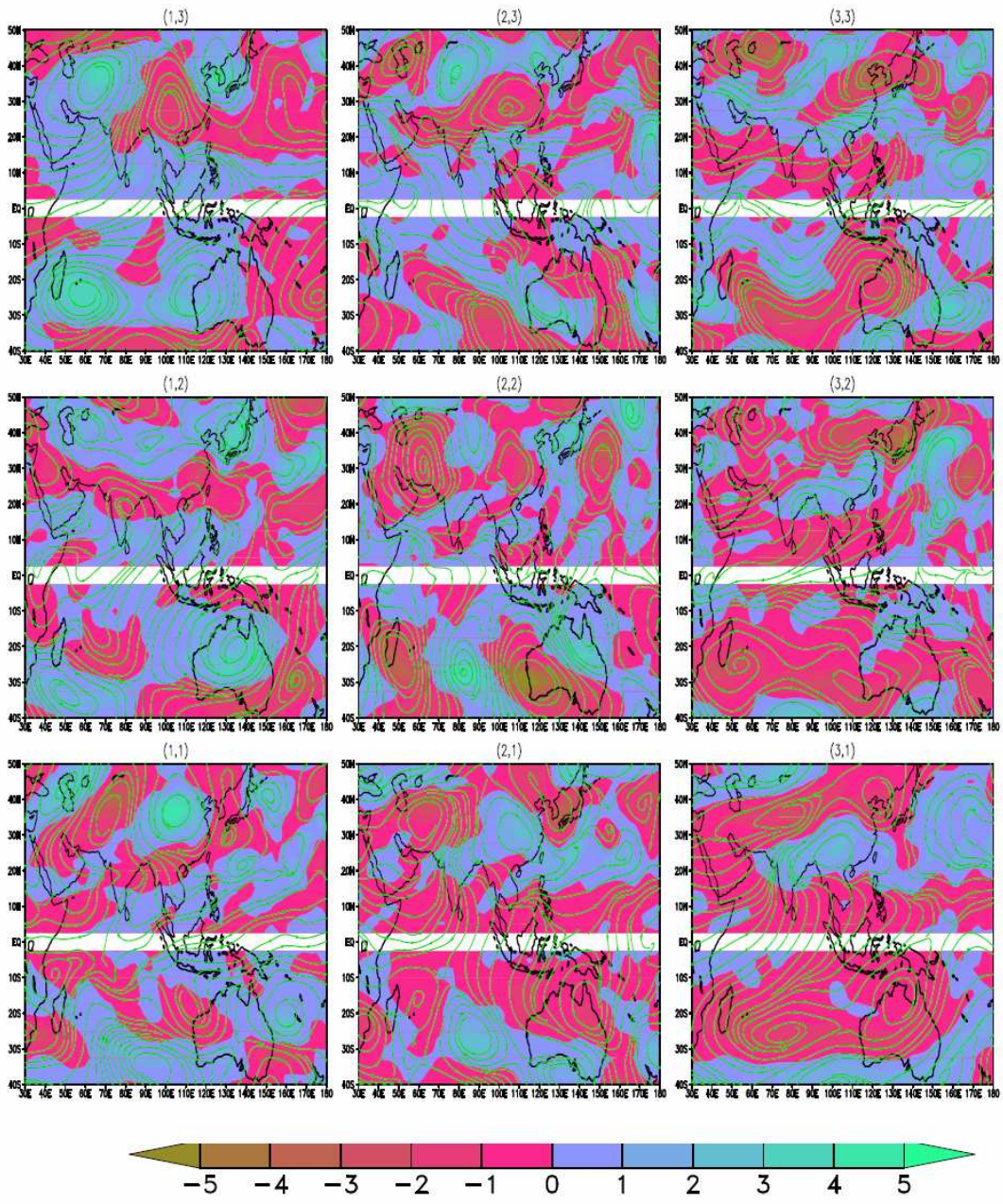

Figure 6: The plot showing the 200hpa anomalous wind streamline and vorticity(shaded).The values of each 3x3 node are the composite anomaly of all the days classified in that node. (units 10**-5/sec)

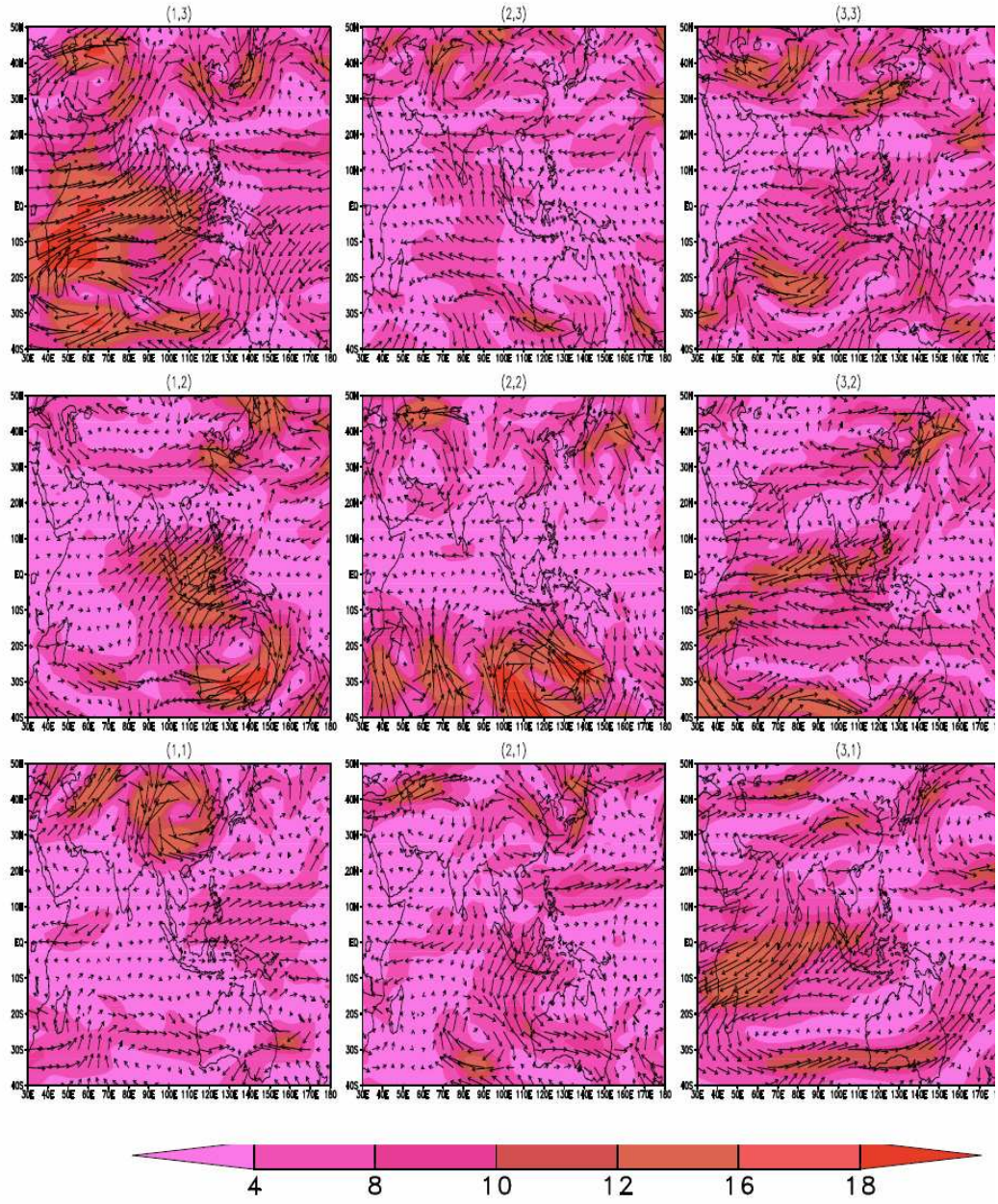

Figure 7: The plot of 200hpa anomalous wind vector and magnitude for all SOM nodes.The values of each 3x3 node are the composite anomaly of all the days classified in that node.(units m/sec)

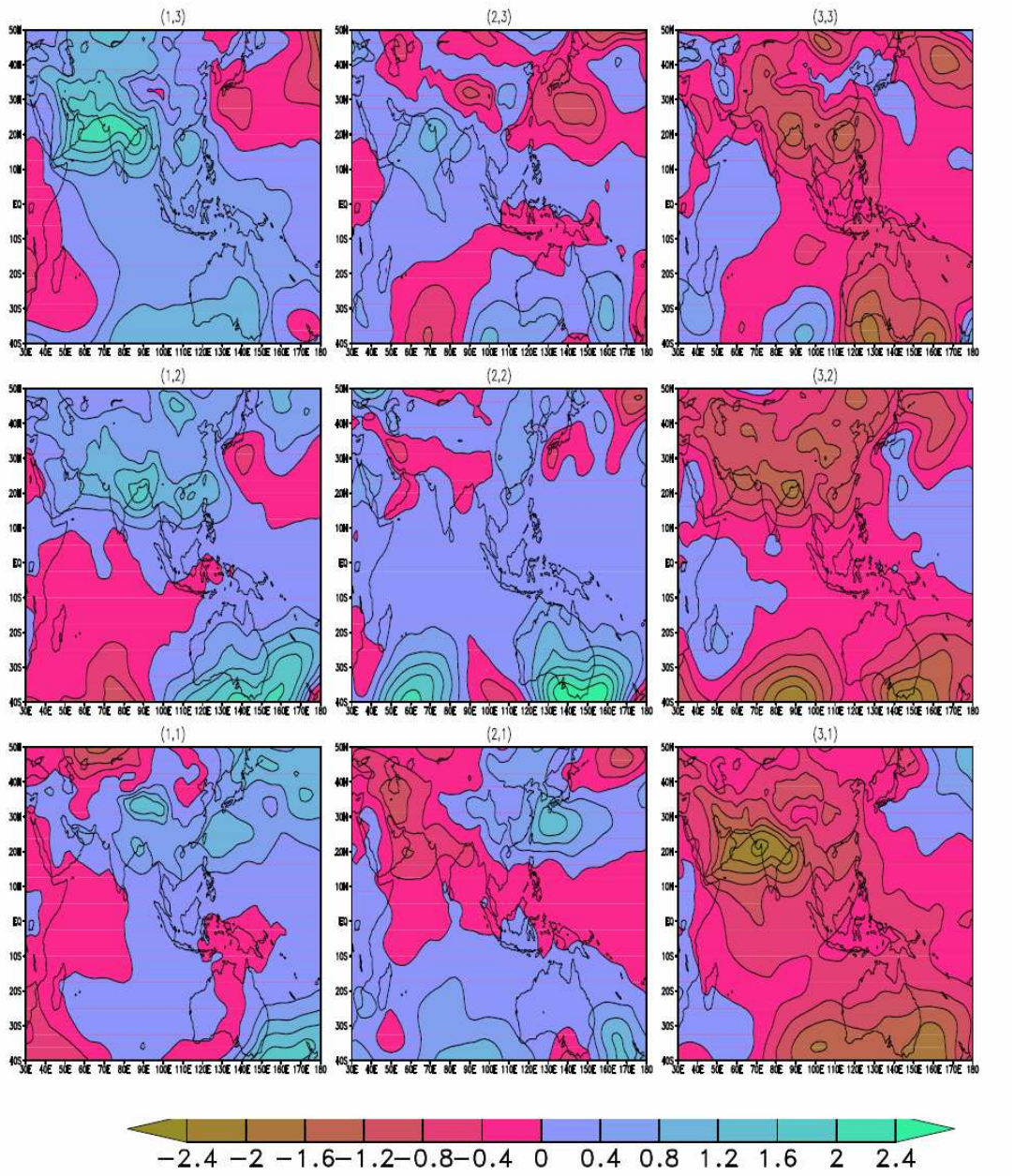

Figure 8: The plot of MSLP anomaly for all SOM nodes.The values of each 3x3 node are the composite anomaly of all the days classified in that node. (units hpa)

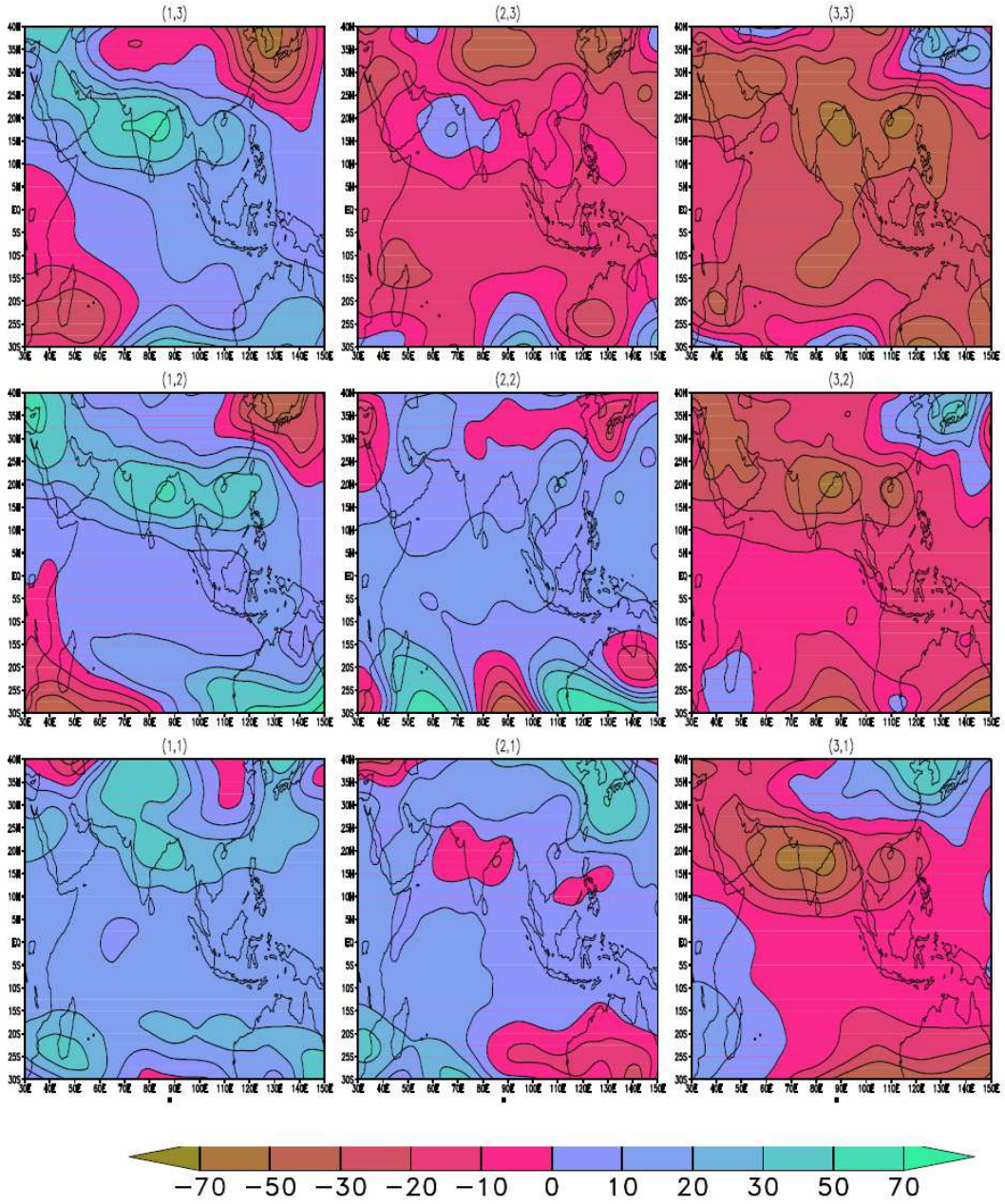

Figure 9: The plot of anomalous geopotential height for all SOM nodes.The values of each 3x3 node are the composite anomaly of all the days classified in that node. (units m)

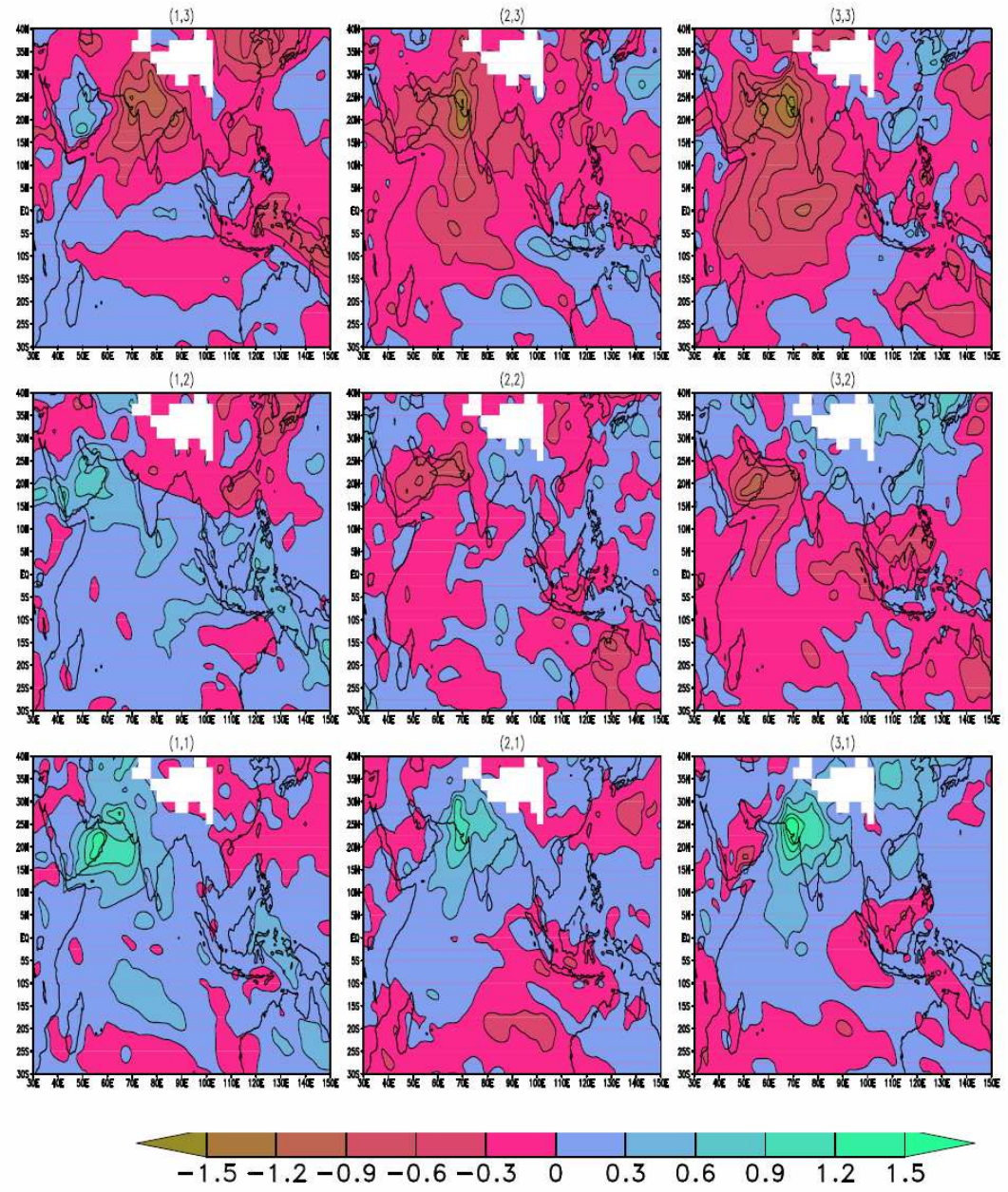

Figure 10: The plot of specific humidity anomaly at 850hpa for all SOM nodes.The values of each 3x3 node are the composite anomaly of all the days classified in that node.(units kg/kg)

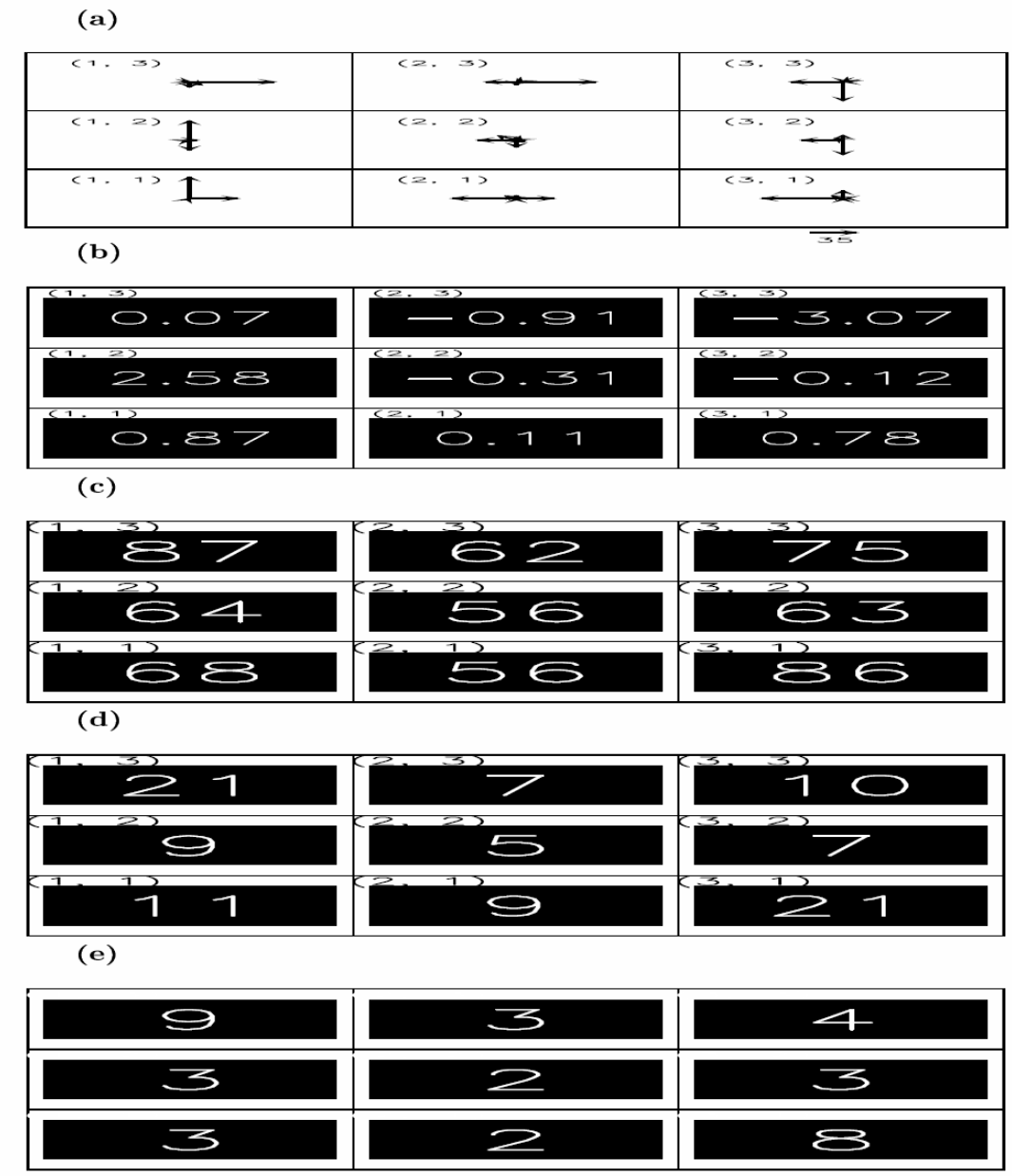

Figure 11: The plot showing for all the SOM nodes:(a)direction of movement (b)trend (c) probability of no transition (d) mean per frequency of days staying at each SOM node (e) mean days per event for the each SOM node.

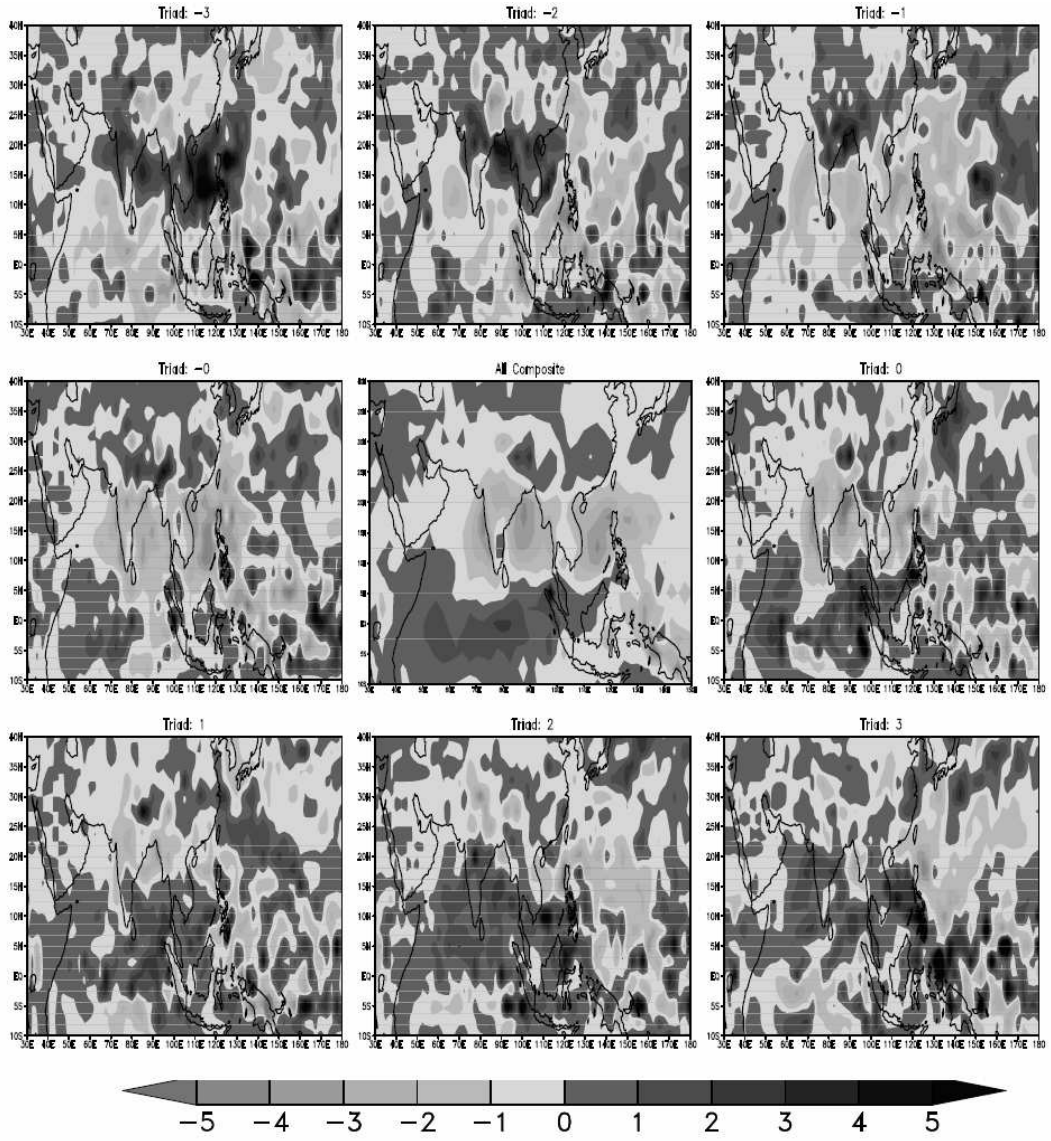

Figure 12: The plot showing the movement node (1,3) or the most break node.

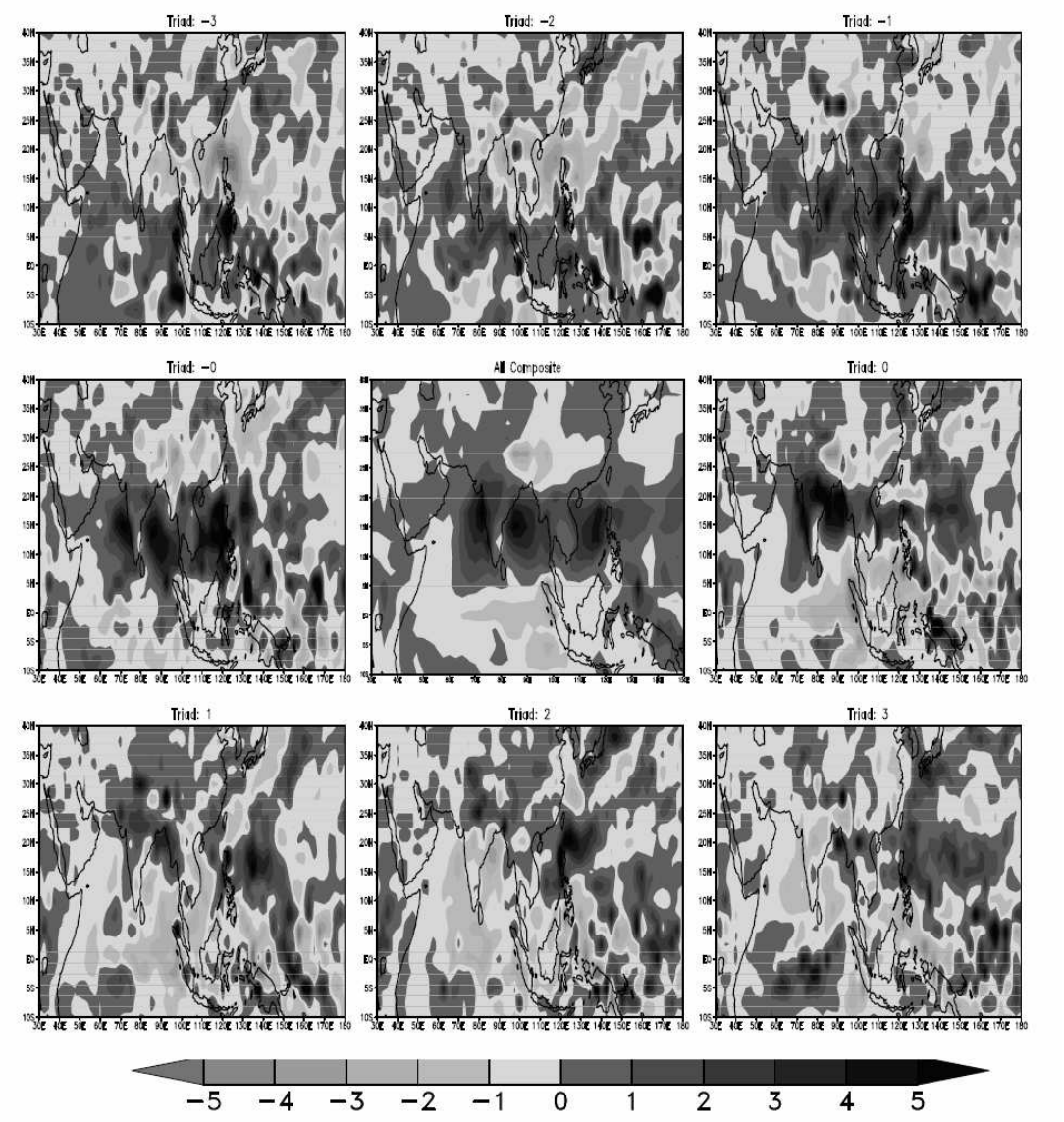

Figure 13: The plot showing the movement node (3,1) or the most active node.

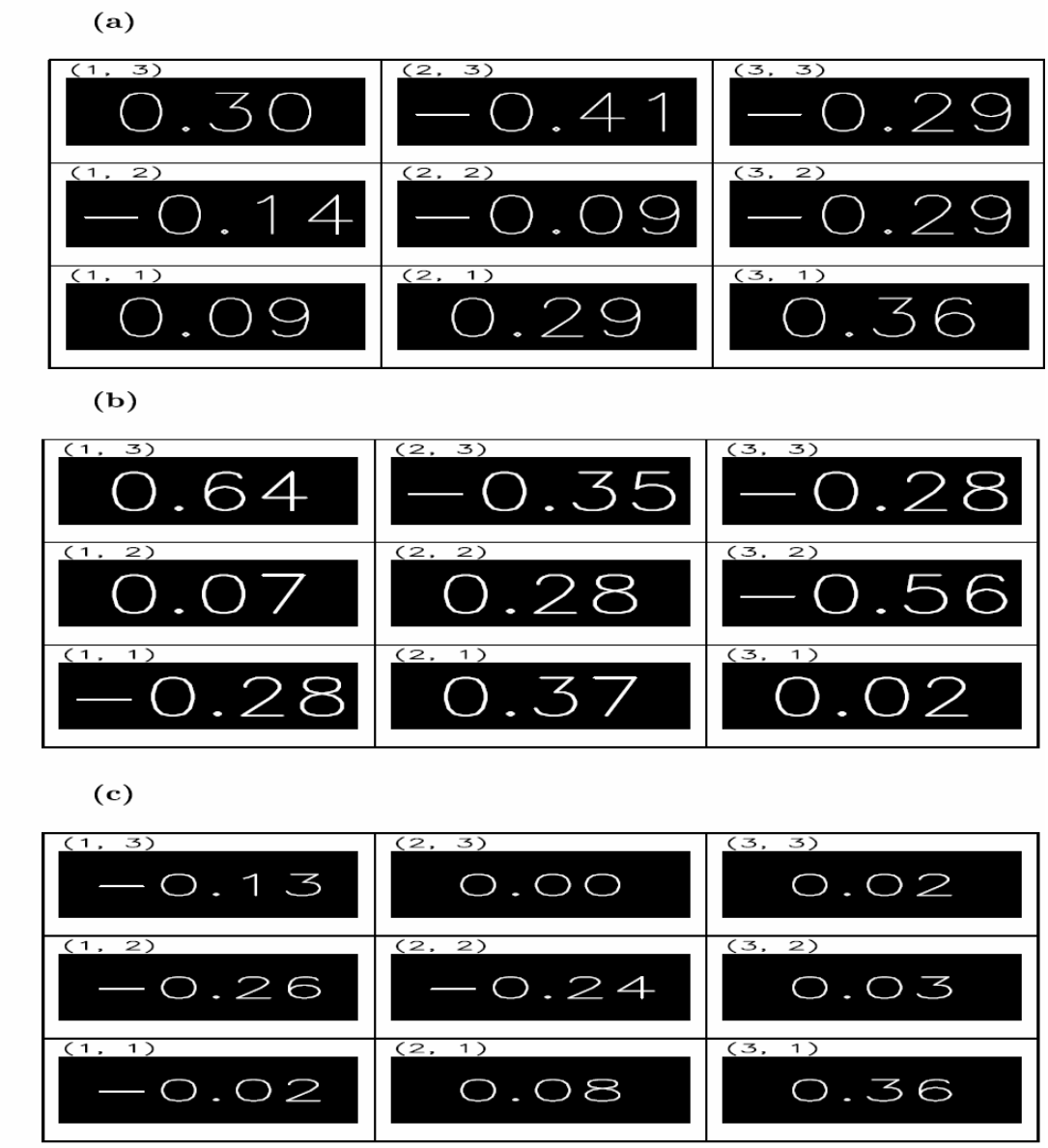

Figure 14: The plot showing the intraseasonal correlation coefficient (a)IOD (b)NINO3 (c) NAO with each SOM node.

(a)

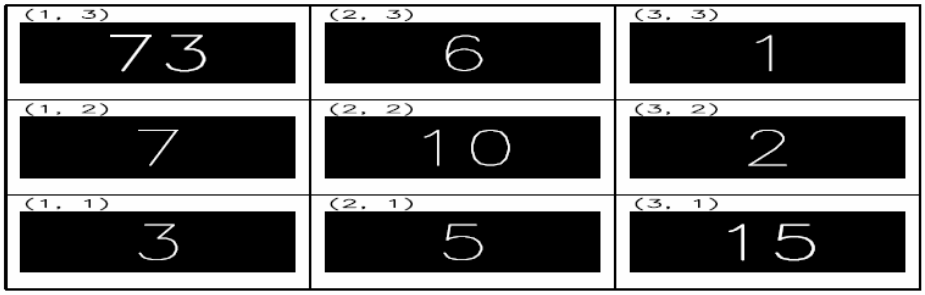

(b)

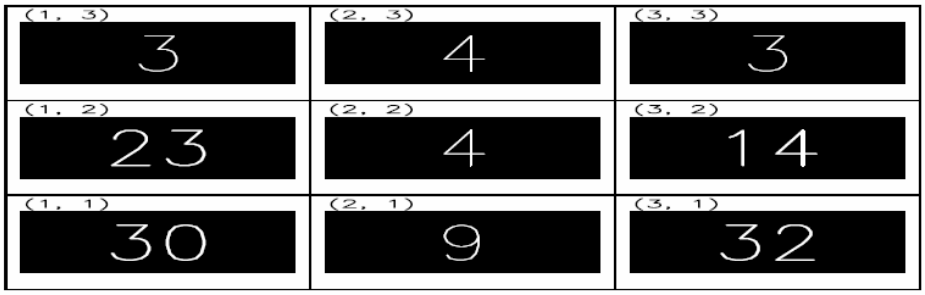

(c)

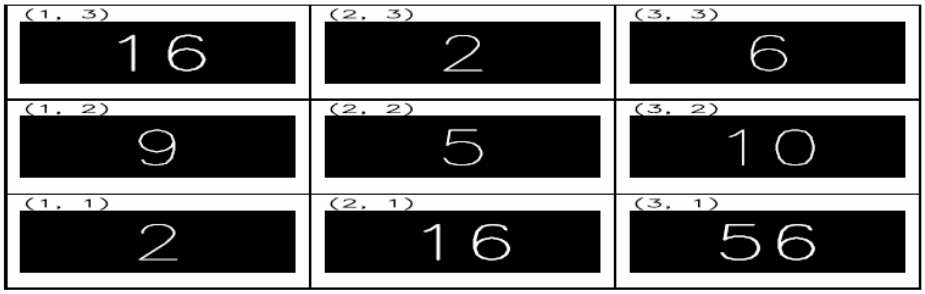

(d)

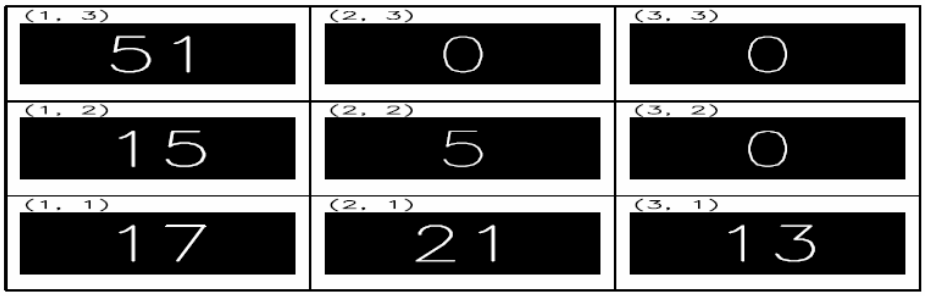

Figure 15: The plot showing the number of active and break days for the years: (a) 1987 (b) 1988 (c) 1994 (d) 1997. The year 1987 is a heavy drought year whereas 1988 is a flood year. The year 1997 is a normal year with severe El-Nino and the year 1994 is an IOD year.

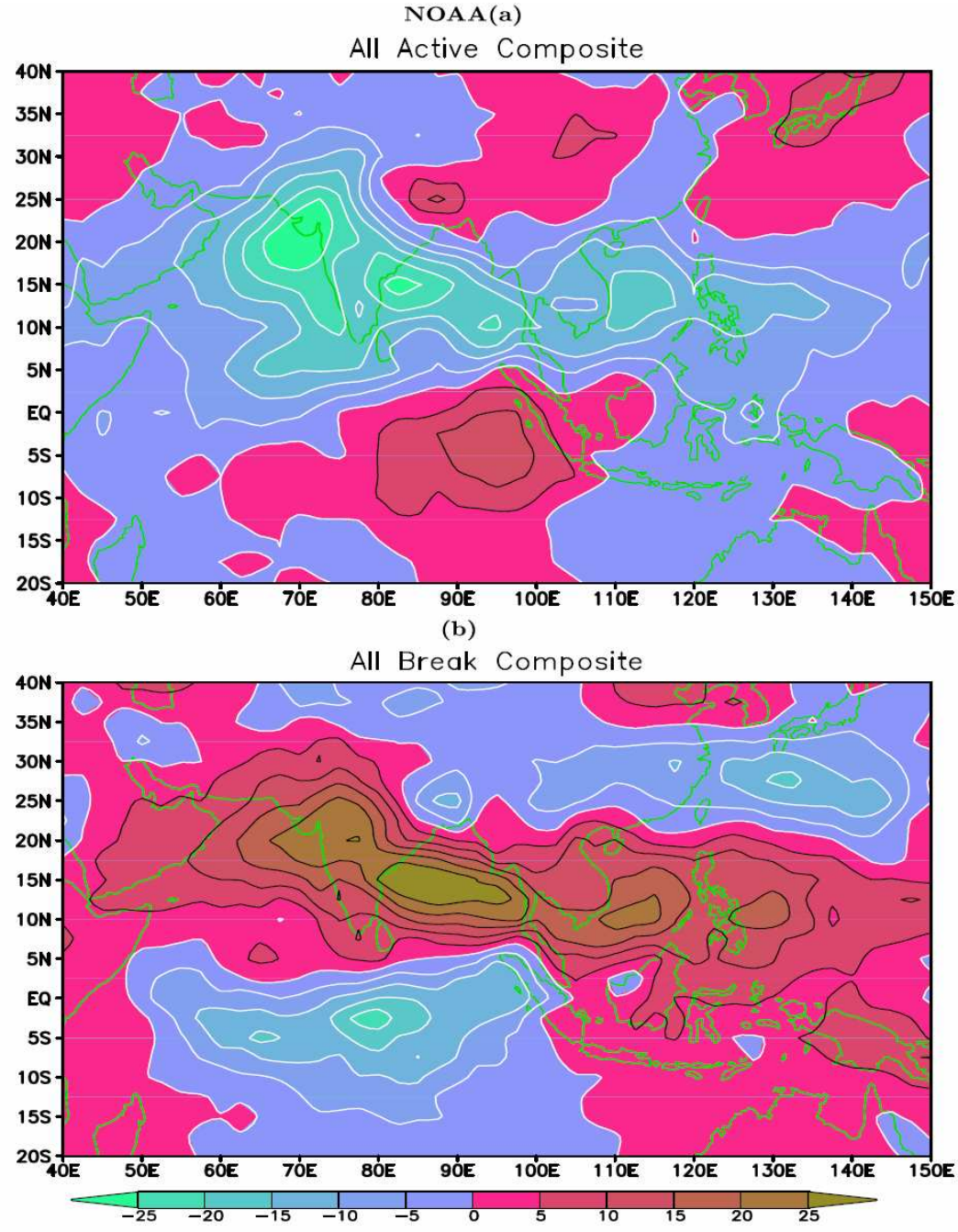

Figure 16: Reconstructed Active and Break Phases from NOAA outgoing longwave radiation data.

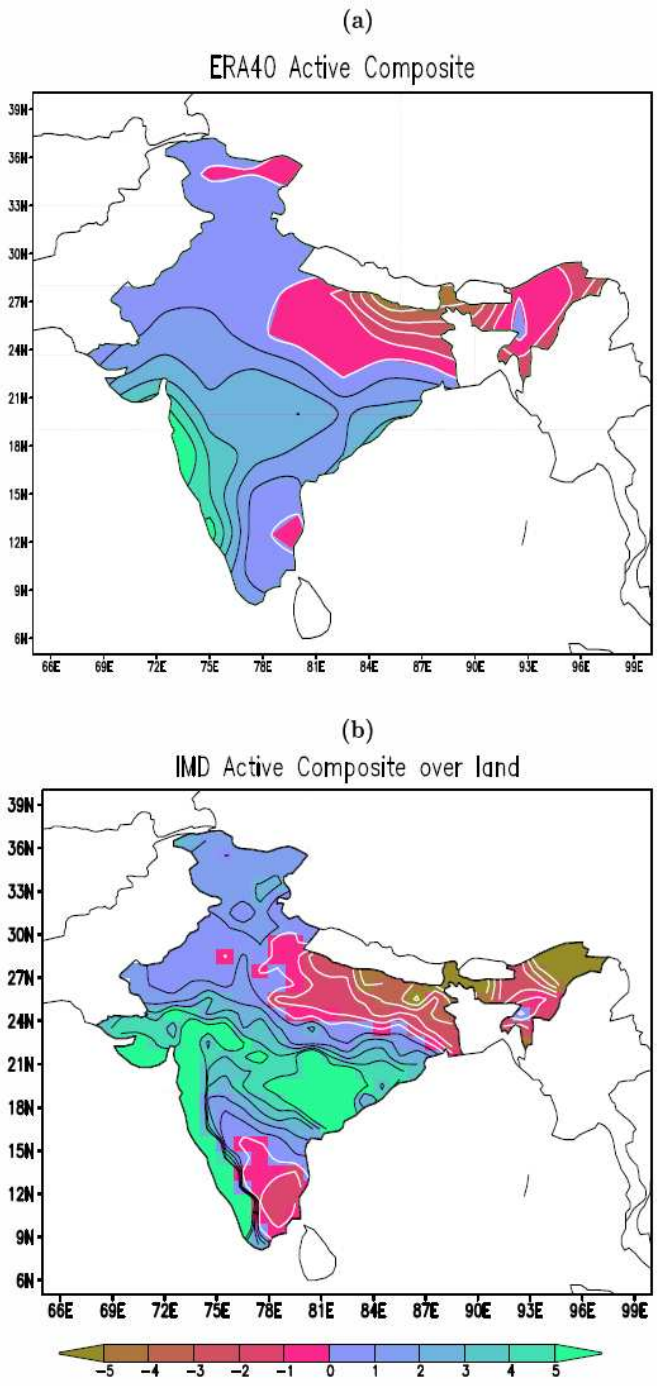

Figure 17: Reconstructed (a) active composite for the ERA-40 rainfall data (b) active composite for the IMD rainfall data. The reconstruction is only over Indian landmass.

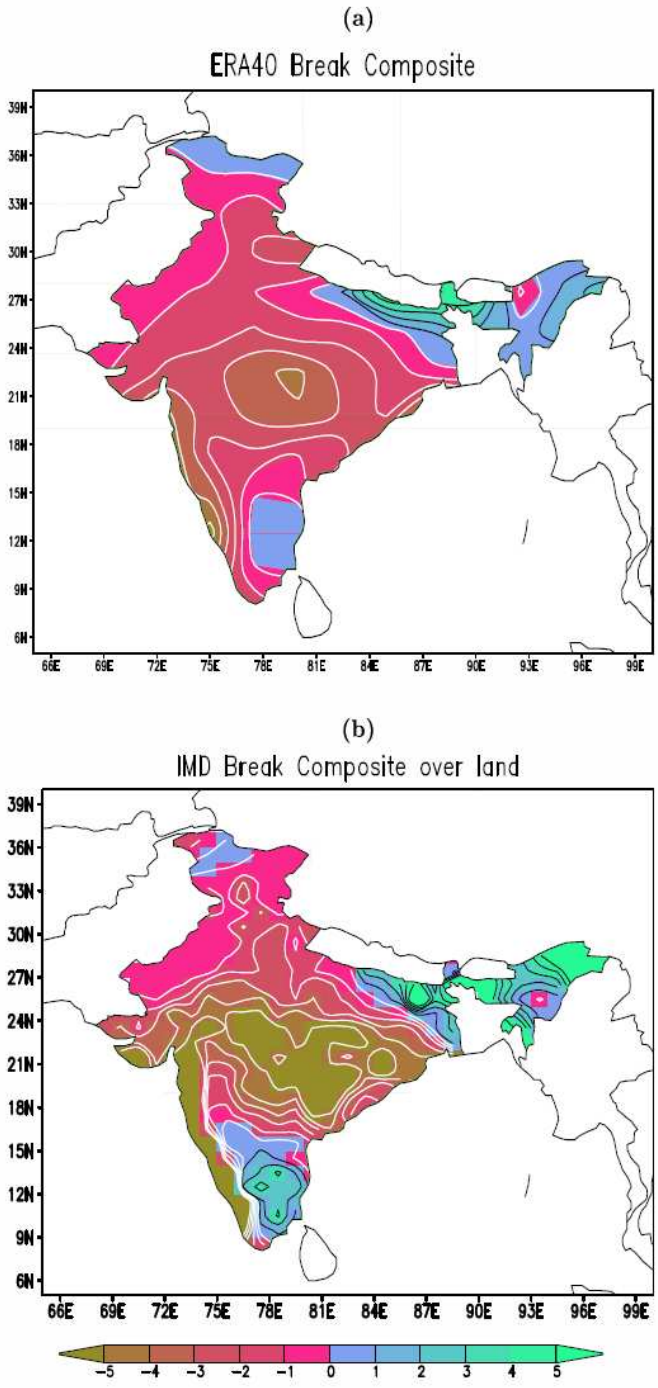

Figure 18: Reconstructed (as fig.17) (a) break composite for the ERA-40 rainfall data (b) break composite for the IMD rainfall data.